Am J Cancer Res 2022;12(6):2492-2525
www.ajcr.us /ISSN:2156-6976/ajcr0141999

Original Article

The homeostatic malfunction of a novel feedback pathway formed by lncRNA021545, miR-330-3p and epiregulin contributes in hepatocarcinoma progression via mediating epithelial-mesenchymal transition

Siwen Yang[1], Yunkun Zhang[1], Chunmei Guo[1], Rui Liu[1], Maroua Elkharti[1], Zhenhua Ge[1], Qinlong Liu[2], Shuqing Liu[1], Ming-Zhong Sun[1]

[1]College of Basic Medical Sciences, Dalian Medical University, Dalian, Liaoning, China; [2]Department of General Surgery, The Second Affiliated Hospital, Dalian Medical University, Dalian, Liaoning, China

Received January 24, 2022; Accepted May 6, 2022; Epub June 15, 2022; Published June 30, 2022

Abstract: A better understanding of tumor metastasis is urgently required for the treatment and prognosis of hepatocarcinoma patients. Current work contributes a novel ceRNA feedback regulation pathway composed of epiregulin (EREG), microRNA-330-3p (miR-330-3p) and long non-coding RNA 021545 (lncRNA021545) in regulating hepatocarcinoma malignancy via epithelial-mesenchymal transition (EMT) process. Closely correlated, the deficiencies of EREG and lncRNA021545 and the overexpression of miR-330-3p were involved in the clinical progression of hepatocarcinoma. *In vitro* results showed that 1) lncRNA021545 downregulation promoted, 2) miR-330-3p dysexpression positively correlated, and 3) EREG dysexpression reversely correlated with the migratory and invasive properties of hepatocarcinoma HCCLM3 and Huh7 cell lines. By directly binding to EREG and lncRNA021545, miR-330-3p expression change reversely correlated with their expressions in HCCLM3 and Huh7 cells, which was also confirmed in primary tumors from HCCLM3-xenograft mice in responding to miR-330-3p change. LncRNA021545 and EREG positively regulated each other, and lncRNA021545 negatively regulated miR-330-3p, while, EREG dysregulation unchanged miR-330-3p expression in hepatocarcinoma cells. Furthermore, systemic *in vitro* cellular characterizations showed that the malfunctions of the three molecules mediated the invasiveness of hepatocarcinoma cells via EMT process through affecting the expressions of E-cadherin, N-cadherin, vimentin, snail and slug, which was further confirmed by *in vivo* miR-330-3p promotion on the tumorigenicity and metastasis of HCCLM3 bearing nude mice and by *in vitro* miR-330-3p promotion on the migration and invasion of hepatocarcinoma cells to be antagonized by EREG overexpression through acting on EMT process. Our work indicates, that by forming a circuit signaling feedback pathway, the homeostatic expressions of lncRNA021545, miR-330-3p and EREG are important in liver health. Its collapse resulted from the downregulations of lncRNA021545 and EREG together with miR-330-3p overexpression promote hepatocarcinoma progression by enhancing the invasiveness of tumor cells through EMT activation. These discoveries suggest that miR-330-3p/lncRNA021545/EREG axis plays a critical role in hepatocarcinoma progression and as a candidate for its treatment.

Keywords: Hepatocarcinoma, EREG, miR-330-3p, lncRNA021545, EMT

Introduction

Primary liver cancer is the sixth most commonly diagnosed cancer and the third leading cause of cancer mortality worldwide in 2020 [1]. Hepatocarcinoma (HCC) is the major histological subtype of liver cancer. HCC can be effectively treated with hepatectomy and liver transplantation, however, the frequent postoperative metastasis leads to high recurrence and poor survival rates of HCC patients, which is also the main obstacle to a full recovery treatment of HCC [2, 3]. New clues to a better understanding of the clinical carcinogenesis and progression, especially the metastasis, are urgently required for improving the diagnosi's, treatment and prognosis of HCC patients.

The epithelial-mesenchymal transition (EMT) refers to the process polarized epithelial cells

lose their characteristics via adhesin, acquire the migratory and invasive properties of mesenchymal cells and enhance their spread and invasion in organs and tissues [4, 5]. EMT plays a vital role in normal organ development and homeostasis [4-8]. It closely involves in the progression and metastasis (especially the migration and invasion) and leads to the harder treatment and worse prognosis of cancers [5, 7-10]. EMT plays a key role in initializing the invasion and metastasis in HCC [5, 6, 11-13]. In HCC carcinogenesis, the overexpressions of the transcription factors including Snail (snail/slug), ZEB (ZEB1/ZEB2) and Twist1 [5, 6, 11] are tightly related with the suppressed expression of E-cadherin, a well-known epithelial marker, with the acquired or increased expressions of N-cadherin and vimentin, the mesenchymal markers [11-13]. However, the metastasis in HCC malignancy is still poorly understood. Accordingly, the study on the new molecular regulation mechanism, especially the upstream triggering event in EMT process, is of particular importance in the carcinogenesis, diagnosis and treatment of HCC. Based on this aim, current work first demonstrated the individual associations of the dysexpressions, with the difference correlations between each two molecules, of epiregulin (EREG), microRNA-330-3p (miR-330-3p) and long non-coding RNA 021545 (lncRNA021545) in cancerous liver tissues with the clinic progression of HCC patients. Further, our cell and molecular biology characterizations showed that the three molecules formed a novel ceRNA regulation mechanism to regulate the migration and invasion properties of hepatocarcinoma cells without affecting their proliferations. The collapse of miR-330-3p/lncRNA021545/EREG feedback regulation due to their expression imbalances enhanced HCC metastasis via activating EMT in hepatocarcinoma malignant progression.

MicroRNAs (miRNAs) are small single strand non-coding RNAs composed of 18~24 nucleotides. The deregulation of miRNAs has been reported in almost all types of human cancers [14-29]. Acting as post transcriptional controllers, miRNAs can inhibit protein translation or damage the mRNAs of targeting genes into fragments. Having been mostly reported so far through binding to the 3'-untranslated regions (UTRs) of target mRNAs, miRNAs exert important roles by degrading or inhibiting the translations of the latters in cancer development and progression [14, 20, 29]. MiR-330-3p is located on chromosome 19q12.32 [15]. Its dysexpression is closely linked to the pathogenesis, proliferation, migration, invasion, prognosis and drug resistance of cancer [16-29]. MiR-330-3p acts as an oncogene in glioma [16], lung cancer [17], esophageal squamous cell carcinoma [18], breast cancer [19] and pancreatic cancer [21]. While, it acts as an anti-oncogene in osteosarcoma [23], gastric [24], ovarian [22] and colorectal [26] cancers. In liver cancer, interestingly and controversially, miR-330-3p was reported to enhance the migration and invasion of HCCLM3 cells via targeting BTG1 [20] and to suppress the migration of HepG2 cells via targeting MAP2K1 [29]. Considering the facts that only one HCC cell line was separately utilized in the above two studies, it is unclear whether this difference arises from the subtype of cancer cell line or not. In current work, miR-330-3p was measured higher expressed in HCC patients' specimens and predicted to promote the progression and poor prognosis of patients. Consistently, the results by using two HCC cell lines, HCCLM3 and Huh7, showed miR-330-3p overexpression and knockdown reversely regulated their migration and invasion properties. Moreover, for the first time, current work further showed, negatively correlated with lncRNA021545 and EREG dysexpressions in HCC patients, miR-330-3p functioned in HCC malignancy through negatively mediated the latter two's expression levels in both cancer cell lines and miR-330-3p bearing nude mice through affecting the EMT process.

Long non-coding RNAs (lncRNAs) are sequences with the size over 200 nucleotides without the function of encoding proteins [30]. LncRNAs function as scaffolds or guides to regulate interactions between proteins and genes, as decoys to bind proteins or miRNAs, and as enhancers to modulate the transcription of their targets after being transcribed from enhancer regions or their neighboring loci [31-33]. LncRNAs play an important role in cell differentiation [34], invasion [35], metabolism [36] and the immune response [37]. LncRNA-021545 is a 3149-bp gene on human chromosome 11 (NONCODE ID: NONHSAT021545.2). Up to now, except for the report of upregulation expression of lncRNA021545 in peripheral

blood of schizophrenic patients [38], the role of lncRNA021545 is still a blank. Herein, we showed, inversely and negatively correlated with miR-330-3p upregulation and EREG deficiency in HCC by forming a ceRNA regulation, lncRNA021545 deficiency promoted HCC progression through enhancing the migratory and invasive behaviours of tumor cells via promoting EMT process.

Locating on human chromosome 4q13.3, epiregulin (EREG) is a member of the epidermal growth factor (EGF) family [39, 40]. It plays a crucial role in drug resistance [41], immune response [42], acute pain [43], angiogenesis [44] and metastasis [45]. EREG has been linked to a variety of cancers [39, 45-50]. The overexpression of EREG favors a better prognosis of patients with rectal [47] and metastatic colorectal cancer [48]. While, it promotes the progression of oral squamous cell carcinoma [45], head and neck squamous cell carcinoma [39] and colon cancer [50]. In the field of liver cancer, EREG-deficient C57Bl/6 mice showed reduced malignancy in DEN plus CCl_4-mediated hepatocarcinogenesis [46] and dual knockdowns of EREG and N-ras affected the growths of HepG2 and Bel7402 cells [49]. Nevertheless, the exact role of EREG in the clinical hepatocarcinogenesis and metastasis remains uncertain. In this work, we first showed EREG was downregulated in hepatocarcinoma cancerous specimens. EREG level changes were further determined to both reversely correlated with the migration and invasion abilities of two HCC cell lines, HCCLM3 and HuH7. Negatively correlated with miR-330-3p and positively correlated with lncRNA02154 expression level changes in malignant tumors, EREG own expression change, as well as with its level change reversely regulated by miR-330-3p and positively regulated by lncRNA021545 expression, which negatively mediates the migration and invasion of HCC cells via EMT process. Moreover, exogenous EREG expression antagonized miR-330-3p enhanced malignant behaviours of HCC cells via affecting EMT process. Again, linked and regulated by miR-330-3p and lncRNA-021545, EREG deficiency contributed to the collapse of miR-330-3p/lncRNA021545/EREG feedback regulation to promote hepatocarcinoma malignancy.

Collectively, our current study revealed a novel ceRNA circuit signaling regulatory pathway composed of EREG, miR-330-3p and lncRNA-021545 in hepatocarcinogenesis and metastasis. The deficiencies of EREG and lncRNA-021545 correlated with miR-330-3p overexpression contributes to the clinical progression of hepatocarcinoma patients by enhancing the migratory and invasive capacities of cancer cells through activating EMT behaviour. Specifically, the collapse of this regulation pathway due to the dysregulation of miR-330-3p, EREG and lncRNA021545 effects the expressions of E-cadherin, N-cadherin, vimentin, snail and slug in hepatocarcinoma cell aggressiveness. It provides a new view in tumor metastasis and a potential clue to the therapeutical treatment of liver cancer.

Materials and methods

Human participants, tissue collection and ethics statement

The paired fresh primary HCC tumor tissues with their respective paracancerous non-tumor liver tissues (> 2.5 cm away from tumorous tissue) from 27 patients were provided by the Second Affiliated Hospital, Dalian Medical University, Dalian, China. There were 21 men and 6 women; 13 patients of age ≥ 60 years and 14 patients of age < 60 years; 10, 11, 5 and 1 patients are in T1, T2, T3 and T4 stages. All participants received no chemo/radiotherapy before surgery. Following surgical resection, the tissue samples were immediately snap frozen in liquid nitrogen and stored at -80°C in prior to use. Informed consent was obtained from each patient. The involvement of human participants and the use of human specimens were evaluated by the Committee of Medical Ethics of Dalian Medical University, ethical number 2019-016. The experiments were rigorously performed according to the permitted guidelines.

Western blotting (WB) assay

Total protein was extracted from tissue or cells using RIPA lysis buffer (Beyotime, China). Protein concentrations were measured by Bradford assay [51] according to the manufacturer's instructions. Equal amounts (30-50 μg) of each protein sample was heated in boiling water for 5 min, separated by 10% SDS-PAGE and transferred onto nitrocellulose (NC) membrane (Millipore, Merck). The NC membrane

Table 1. Synthesized primers for targeting molecules

Molecule	Sequence
EREG	F: 5'-GGACAGTGCATCTATCTGGTGGA-3'
	R: 5'-AGTGTTCACATCGGACACCAGTA-3'
lncRNA021545	F: 5'-CAGATGGTTCAAAAGTGCAAT-3'
	R: 5'-TAAAGCCAGATACTCCCAAGGAC-3'
U6	F: 5'-CTCGCTTCGGCAGCACA-3'
	R: 5'-AACGCTTCACGAATTTGCGT-3'
ACTB	F: 5'-AGGCCAACCGCGAGAAG-3'
	R: 5'-ACAGCCTGGATAGCAACGTACA-3'

EREG, epiregulin; lncRNA021545, long non-coding RNA 021545; ACTB, β-actin; F, Forward; R, Reverse.

was then blocked with 5% skim milk (BD, USA) in TBST buffer for 2 h at room temperature (RT) and then incubated with primary antibodies at 4°C overnight. The primary antibodies were EREG (1:800, ab233512, Abcam, USA), snail (1:800, 13099-1-AP, ProteinTech, China), slug (1:1000, 12129-1-AP, ProteinTech, China), E-cadherin (1:800, 20874-1-AP, ProteinTech, China), N-cadherin (1:1000, 22018-1-AP, ProteinTech, China), vimentin (1:1500, 10366-1-AP, ProteinTech, China), GAPDH (1:5000, 10494-1-AP, ProteinTech, China). The NC membrane was washed with TBST for 3 × 10 min, incubated with the anti-rabbit IgG (1:5000, SA00001-2, ProteinTech, China) for 1 h at RT and washed with TBST for 3 × 10 min. Protein bands were visualized by electrochemiluminescence (ECL, Advansta, USA) and analyzed using a ChemiDoc™ MP system (Bio-Rad, USA). The *t*-test method was used to compare differential expression level of proteins.

Cell culture

Human hepatocarcinoma HuH7 and HCCLM3 cell lines were obtained from Shanghai Institute of Biochemistry and Cell Biology, Chinese Academy of Sciences, China and maintained in our laboratory. Genotyping analyses using an ABI 3730xl genetic analyzer showed no multiple alleles and mutations found in the two cell lines in prior to the designed experiments. Huh7 and HCCLM3 cells were incubated in 10% fetal bovine serum (FBS) (ExCell Bio, China) supplemented with 100 U/mL of penicillin and 100 U/mL streptomycin (Gibco, USA) in Dulbecco's modified Eagle's medium (DMEM, Gibco, USA) in a humidified incubator (HERAcell 150i, ThermoFisher, USA) with 5% CO_2 at 37°C.

RNA isolation and quantitative real-time PCR (qRT-PCR) assay

The total RNA was either extracted from experimental cells or tissues by Trizol™ reagent (TransGen, China) and reversely transcribed into cDNA using EasyScript One-Step gDNA Removal and cDNA Synthesis SuperMix kits (TransGen, China). qRT-PCR was performed using a TransStart Tip Green qPCR SuperMix kit (TransGen, China) with a StepOnePlus™ Real-Time PCR system (ThermoFisher, USA). snRNA U6 was used as internal reference for miR-330-3p and β-actin (*ACTB*) was used as the internal reference for EREG and lncRNA-021545, respectively. The primers for lncRNA-021545, *EREG*, U6 and β-actin were synthesized as in **Table 1**. MiR-330-3p primer sequences were designed by company with the production number of MQPS0001068-1-200 (RiboBio, China). The relative expression differences of targeting molecules were quantified and compared using the $2^{-\Delta\Delta CT}$ method [52].

miR-330-3p overexpression by mimic transfection and downregulation by inhibitor transfection

2×10^5 HuH7 and HCCLM3 cells in 2 mL DMEM with 10% FBS without antibiotic were seeded into a 6-well plate and cultured at 37°C with 5% CO_2 for 24 h. 4 μL of each of miR-330-3p mimic (50 nM), inhibitor (50 nM) or negative control miRNA (miR-NC, 50 nM) was mixed well with 46 μL DMEM as solution 1 and put at RT for 5 min. 4 μL lipofectamine™ 2000 (ThermoFisher, USA) was mixed well with 46 μL DMEM as solution 2 and put at RT for 5 min. Then, solution 1 was mixed with solution 2 and placed still at RT for 20 min. The corresponding transfection reagent was added into each group cells drop by drop. The cells were first preserved at 37°C with 5% CO_2 for 6-8 h and then were continuously cultured for 48 h following the culture medium with 10% FBS in DMEM. The cells transiently transfected with miR-NC, miR-330-3p mimic, miR-330-3p inhibitor were named as HuH7-miR-NC, HuH7-miR-330-3p-mimic, HuH7-miR-330-3p-inhibitor, HCCLM3-miR-NC, HCCLM3-miR-330-3p-mimic and HCCLM3-miR-330-3p-inhibitor, respectively.

Table 2. Sequences of siRNA used for EREG and lncRNA021545 knockdown

Molecule	siRNA duplex oligoribonucleotide sequence
siEREG-1	F: 5'-GCUCAAGUGUCAAUAACAATT-3'
	R: 5'-UUGUUAUUGACACUUGAGCTT-3'
siEREG-2	F: 5'-CCACCAACCUUUAAGCAAATT-3'
	R: 5'-UUUGCUUAAAGGUUGGUGGTT-3'
siEREG-3	F: 5'-GUACAGAAAUCGAAAAAGUTT-3'
	R: 5'-ACUUUUUCGAUUUCUGUACTT-3'
silncRNA021545-1	F: 5'-GCACCAAUCAACUACUUAUTT-3'
	R: 5'-AUAAGUAGUUGAUUGGUGCTT-3'
silncRNA021545-2	F: 5'-GCACAAACAUAGAGCCAAATT-3'
	R: 5'-UUUGGCUCUAUGUUUGUGCTT-3'
siNC	F: 5'-UUCUCCGAACGUGUCACGUTT-3'
	R: 5'-ACGUGACACGUUCGGAGAATT-3'

EREG knockdown by siRNA interference and overexpression by lentivirus transfection

EREG knockdown: As shown in **Table 2**, three small interfering RNAs to *EREG* (Genbank: NM_001432) were designed using Invitrogen, siDirect and Whitehead softwares to knockdown EREG in cells by transfection with lipofectamine™ 2000. Briefly, 2 × 10^5 HuH7 and HCCLM3 cells in 2 mL DMEM with 10% FBS without antibiotic were seeded into a 6-well plate and incubated at 37°C with 5% CO_2 for 24 h. Then, 2.5 μL of each of siEREG-1 (20 μM), siEREG-2 (20 μM) and siEREG-3 (20 μM) or 7.5 μL small interfering RNA-negative control (siNC, 20 μM) was mixed well with 42.5 μL DMEM and placed at RT for 5 min. At the same time, 6 μL lipofectamine™ 2000 (ThermoFisher, USA) was mixed well with 44 μL DMEM and placed still at RT for 5 min. The rest steps were the same as described above.

EREG overexpression: To overexpress EREG in HCCLM3 cells, the full-length coding sequence of *EREG* was first amplificated by PCR using its forward primer 5'-GCTCTAGAGCCACCTCAGAGGGACACAGCCAAC-3' and reverse primer 5'-CCGGAATTCGACCTAACACTTGACCCAACA-3', then cloned into the *Xba* I and *EcoR* I sites of PCDH-EF1-MCS-T2A-Puro vector (PCDH). The recombinant PCDH-EF1-MCS-T2A-Puro-EREG (PCDH-EREG) expression vector was used for overexpressing EREG in HCCLM3 cells. The empty vector PCDH was also transfected into HCCLM3 as the control cells.

Lentivirus production and HCCLM3 cell infection were performed according to the manufacturer's instruction. 1 × 10^5 293 T cells in 2 mL DMEM with 10% FBS without antibiotic were seeded into a 6-well plate and incubated at 37°C with 5% CO_2 for 24 h. Then, 1.5 μg PCDH-EREG or PCDH combined with 1.5 μg packaging plasmids including psPAX2 and pMD2G were separately mixed with DMEM with a final volume of 50 μL and placed at RT for 5 min. Meanwhile, 3 μL lipofectamine™ 2000 (ThermoFisher, USA) was mixed well with 47 μL DMEM and placed still at RT for 5 min. The rest steps were the same as described above. At the transfection time intervals of 24 and 48 h, the virus particle supernatants were first centrifugating at 5000 rpm for 10 min followed by filtering through 0.22 μm microporous membrane (Millipore, USA). 1 × 10^5 HCCLM3 cells from each group in a well of 6-well plates were infected with 1 mL lentivirus and 1 mL 10% FBS in DMEM containing 8 μg/mL polybrene (Solarbio, China) at 37°C with 5% CO_2 for 48 h. The cells stably transfected with PCDH-EREG or the PCDH vector were screened against with the concentration gradients of 0.1, 0.2 and 0.4 μg/mL puromycin (Coolaber Science & Technology, China) at 37°C with 5% CO_2 with a duration for about 6 months to obtain the HCCLM3-PCDH-EREG and HCCLM3-PCDH cells.

LncRNA021545 knockdown by siRNA interference

To knockdown lncRNA021545 in cells, as shown in **Table 2**, two small interfering RNAs to lncRNA021545 (NONCODE ID: NONHSAT021545.2) were synthesized. 2 × 10^5 HuH7 or HCCLM3 cells in 2 mL 10% FBS in DMEM were seeded into a 6-well plate and incubated at 37°C with 5% CO_2 for 24 h. Then, 3.5 μL silncRNA021545-1 (20 μM) and 3.5 μL silncRNA021545-2 (20 μM) or 7 μL siNC (20 μM) was mixed well with 43 μL DMEM and placed at RT for 5 min, meanwhile, 6 μL lipofectamine™ 2000 (ThermoFisher, USA) was mixed well with 44 μL DMEM and also placed at RT for 5 min. The remaining steps were carried out as described previously.

Luciferase reporter gene assay

The luciferase reporter gene assay measured the binding sites between miR-330-3p and *EREG* as well as between lncRNA021545 and *EREG*. The pmirGlO expression vector was used to provide the constitutive expression of firefly luciferase as an internal reference. 1 × 10^5 HCCLM3 cells/well were seeded into a 24-well plate in 1 mL 10% FBS in DMEM and incubated at 37°C with 5% CO_2 for 24 h. 1.5 μg of each of the constructed plasmids for both wild type and mutated EREG and lncRNA021545, pmirGlO-EREG-3'-UTR-WT, pmirGlO-EREG-3'-UTR-MUT, pmirGlO-lncRNA0-21545-WT and pmirGlO-lncRNA021545-MUT were co-transfected along with miR-330-3p mimic (1 μL of 50 nM) into HCCLM3 cells using lipofectamine™ 2000 (ThermoFisher, USA). In 24 h following transfection, the cells were washed well with PBS buffer, lysed in 100 μL passive lysis buffer (PLB) with shaking for 15 min at RT. The lysate was transferred into a luminometer tube, mixed well with 50 μL of luciferase assay reagent II (LAR II) first for Firefly luciferase activity assay, then mixed with 100 μL of stop reagent for Renilla luciferase activity assay. Luciferase activity was determined using a GloMax fluorescence reader (Promega, CA, USA).

Cell proliferation by MTT assay

The influences of the dysexpressions of miR-330-3p, EREG and lncRNA021545 on the *in vitro* proliferations of HuH7 and HCCLM3 cells were measured using the microculture tetrazolium test (MTT) assay. Briefly, 1000 of each HuH7 and HCCLM3 group cells in 200 μL DMEM supplemented with 10% FBS were seeded into a well of 96-well plate and incubated at 37°C with 5% CO_2. At the incubation time intervals of 24, 48, 72, 96 and 120 h, 100 μL of MTT solution (5 mg/mL) was separately added into each well by replacing culture medium and incubated further in the dark at 37°C with 5% CO_2 for 4 h. Following the careful removal of the supernatant, 150 μL of dimethylsulfoxide (DMSO, Sigma, USA) was pipetted into each well to dissolve the formazan crystals. The absorbance at 492 nm was measured using a microplate reader (ThermoFisher, USA). The results from triplicate experiments were then quantitatively analyzed.

Boyden transwell chamber assays of cell migration and invasion

24-well-plate transwell chamber assays were performed to investigate the deregulations of miR-330-3p, EREG and lncRNA021545 on the *in vitro* migration and invasion abilities of HuH7 and HCCLM3 cells. 2 × 10^4 cells in 200 μL serum free DMEM were seeded onto the upper chamber of polycarbonate filter unit with 8 μm pore size in 24 well plate (Corning, USA). The chamber was transferred into each well containing 600 μL DMEM with 15% FBS and incubated at 37°C with 5% CO_2 for 24 h. For invasion assay, each filter in the upper chamber was first coated with 50 μL extracellular matrix gel (ECM, Sigma, USA) that was 1:39 diluted with DMEM by incubating at 37°C for 1 h. The non-migrated or non-invaded cells on the upper surface of the insert were removed by swabbing. The migrated or invaded cells to the lower membrane surface were fixed with methanol (Sinopharm Chemical Reagent Co, China) for 30 min, stained with 0.1% crystal violet for 30 min, and washed with PBS twice. Five field views were randomly selected to calculate an average cell count using an upright light microscope (BX63, Olympus, Japan) with 200 ×.

miR-330-3p affects in vivo tumorigenicity and lymph node metastasis of HCCLM3 in nude mice

Nude mouse xenograft was performed to investigate the dysexpression of EREG on the *in vivo* tumorigenicity and lymph node metastasis (LNM) of HCCLM3 cells. 21 male BALB/c-nude mice (4-6 w) were randomly divided into 3 groups with 7 mice per group. 2 × 10^6 of each HCCLM3-miR-NC, HCCLM3-miR-330-3p-mimic and HCCLM3-miR-330-3p-inhibitor group cells in 200 μL DMEM with 15% FBS were subcutaneously injected into the left abdomen of a mouse. The length and width of the tumor xenografts were preciously measured using a caliper in mm once every third days. The tumor volume (V) was calculated according to V = 1/2 × length × $width^2$. On the 20^{th} day after implantation, the primary tumorous xenografts, inguinal and pararenal LNs were immediately dissected from euthanized mice, weighed, appropriately stored in prior to use. About 1/3 of each tumorous tissue was cut and frozen in liquid nitrogen for RNA extraction. The remain-

ing tumorous tissues and LNs were fixed in 10% neutral formalin at RT for 24 h, and em bedded in paraffin, sectioned into 3-5 μm slices, either for IHC or HE assay or for both assays. Nude BALB/c mice were supplied by the SPF Animal Model Center of Dalian Medical University. The study was performed following the ethical standards of the national and international guidelines with the approval of the Experiment Animal Ethical Committee of Dalian Medical University.

Hematoxylin eosin (HE) staining assay

The paraffin sections were dewaxed with xylene for 2 × 5 min, rehydrated with a gradient (100%, 5 min; 95%, 2 min; 85%, 2 min; 75%, 2 min) of ethanol and distilled water for 2 min. The sections were stained in hematoxylin dyeing solution (Sangon Biotechnology Co, China) for 10 min and washed with running tap water for 5 min, differentiated in differentiation solution for 30 s, soaked in water for 15 min, subsequently stained in eosin staining solution (Sangon Biotechnology Co, China) for 30 s, rinsed with running water and immersed in distilled water for 5 min. Then, the sections were dehydrated with ethanol gradient (75%, 2 min; 85%, 2 min; 95%, 2 min, 100%, 5 min), cleared with xylene, sealed with neutral gum (Sinopharm Chemical Reagent Co, China). Slides were examined and imaged under BX63 optical microscope (Olympus, Japan) at 100 × and 400 ×, respectively.

Immunohistochemistry (IHC) assay

IHC assay was performed using an immunohistochemistry kit (ZSGB-BIO, China) to analyze the expression levels of EREG, snail, slug, E-cadherin, N-cadherin, vimentin and Ki-67 in tumorous tissues from HCCLM3-miR-NC, -miR-330-3p-mimic and -miR-330-3p-inhibitor cells transplanted nude mice. Having been dewaxed and rehydrated as above, the slices were further merged in 3% H_2O_2 for 10 min, blocked in 10% non-immune goat serum for 10 min and incubated with the primary antibodies including EREG (1:100, PA5-46969, ThermoFisher, USA), snail (1:300, ABP0121, Abbkine, USA), slug (1:800, 12129-1-AP, ProteinTech, China), E-cadherin (1:1000, 20874-1-AP, ProteinTech, China), N-cadherin (1:2000, 22018-1-AP, ProteinTech, China), vimentin (1:3000, 10366-1-AP, ProteinTech, China), Ki-67 (1:400, 27309-1-AP, ProteinTech, China) at 4°C overnight. The slides were then washed with PBS, incubated with peroxidase-conjugated streptavidin at 37°C for 15 min, washed with PBS for 3 times in prior to color development by diaminobenzidine (DAB) at RT. The slides were counterstained with hematoxylin, dehydrated by gradient ethanol (75%, 2 min; 85%, 2 min; 95%, 2 min, 100%, 5 min), clarified by xylene and sealed with neutral gum. The stained slides were then loaded into an Aperio GT450 (Leica, Germany) system for image scan. An Aperio eSlide Manager software automatically reads the images with dark brown for strong positive, brown for moderate positive, light yellow for weak positive and blue nuclei for negative immunoactivities, as well as analyzed the percentage of each stained area and calculated the Histoscore (H-score).

Data processing and statistical analysis

The results were presented as mean ± SD. Data analysis was performed by utilizing GraphPad Prism 6.0 software (La Jolla, USA). Comparisons between the groups were analyzed by Student's *t*-test. The correlation among the expression of EREG, miR-330-3p and lncRNA021545 were analyzed using the Spearman's rank correlation coefficient. *, **, *** and **** refer to the *P* values of the differences were below 0.05, 0.01, 0.001 and 0.0001, respectively. ns refers to no statistical significance.

Results

The expression changes with their correlations of EREG, miR-330-3p and lncRNA021545 in HCC patients' tumors

The expression level changes of EREG, miR-330-3p and lncRNA021545 were measured in tumorous tissues compared with their paired paracancerous non-tumor tissues from HCC patients. WB results showed, although comparable and upregulated EREG expressions were detected in 4/27 of patients' tumorous tissues compared with their non-tumor liver tissues, EREG was detected in the majority (18/27) of patients' tumorous tissues with an overall decrease of ~40.8% with statistical significance ($P < 0.0001$, **Figure 1A**). As shown in **Figure 1B**, miR-330-3p expression was measured increased by 70.8% ($P = 0.0359$) in

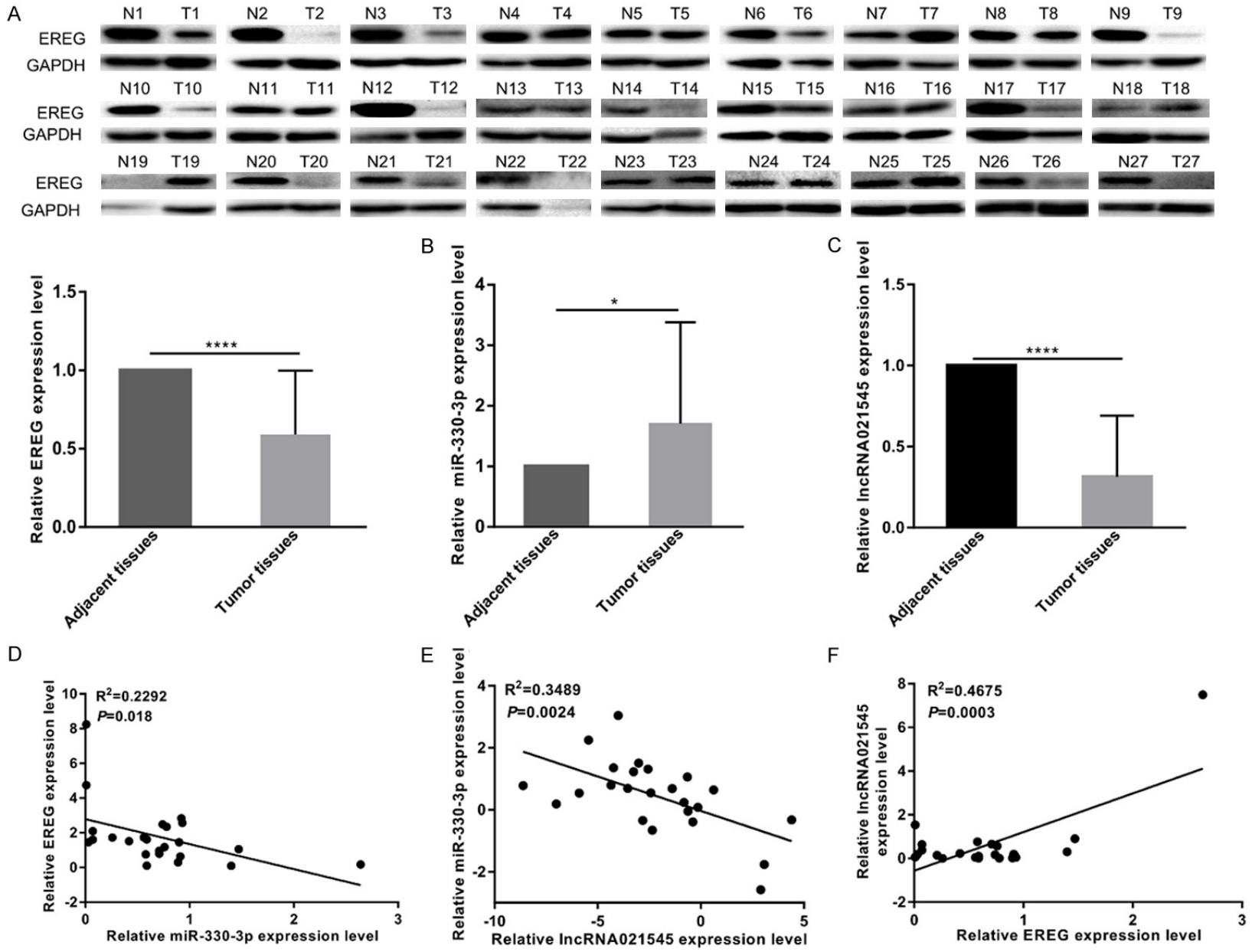
A
N1 T1 N2 T2 N3 T3 N4 T4 N5 T5 N6 T6 N7 T7 N8 T8 N9 T9
EREG
GAPDH
N10 T10 N11 T11 N12 T12 N13 T13 N14 T14 N15 T15 N16 T16 N17 T17 N18 T18
EREG
GAPDH
N19 T19 N20 T20 N21 T21 N22 T22 N23 T23 N24 T24 N25 T25 N26 T26 N27 T27
EREG
GAPDH
B
Relative EREG expression level
****
Adjacent tissues
Tumor tissues
C
Relative miR-330-3p expression level
*
Adjacent tissues
Tumor tissues
D
Relative lncRNA021545 expression level
****
Adjacent tissues
Tumor tissues
E
Relative EREG expression level
R2=0.2292
P=0.018
Relative miR-330-3p expression level
F
Relative miR-330-3p expression level
R2=0.3489
P=0.0024
Relative lncRNA021545 expression level
Relative lncRNA021545 expression level
R2=0.4675
P=0.0003
Relative EREG expression level

Figure 1. The expression changes with their correlations of EREG, miR-330-3p and lncRNA021545 in HCC tumorous tissues. (A) WB assay showed the overall EREG expression was downregulated in tumorous tissues from HCC patients compared with the paired paracancerous non-tumor liver tissues. qRT-PCR showed miR-330-3p (B) was upregulated and lncRNA021545 (C) was downregulated in patients' tumorous tissues. EREG (D) and LncRNA021545 (E) decreases were negatively correlated with miR-330-3p increase and (F) EREG and lncRNA021545 reductions were positively correlated in HCC tissues.

patients' tumorous tissues. LncRNA021545 was measured downregulated by 68.7% ($P < 0.0001$, **Figure 1C**) in patients' tumorous tissues. These results implicated the clinical involvement of the deficiencies of EREG and lncRNA021545 and the overexpression of miR-330-3p in HCC progression. At the same time deserving more attention was the inter-correlations of EREG, miR-330-3p and lncRNA021545 expression changes in HCC tumorous tissues. The overexpression of miR-330-3p in tumorous tissues was both inversely correlated with the reductions of EREG ($R^2 = 0.2292$, $P = 0.018$, **Figure 1D**) and lncRNA021545 ($R^2 = 0.3489$, $P = 0.0024$, **Figure 1E**). The deficiencies of EREG and lncRNA021545 were revealed positively correlated in tumors ($R^2 = 0.4675$, $P = 0.003$, **Figure 1F**). The above results showed that EREG, miR-330-3p and lncRNA021545, with mutual regulatory relationship among them, were related to hepatocarcinoma malignancy.

miR-330-3p directly targets and negatively regulates EREG and lncRNA021545 expressions

The bindings between *EREG* and miR-330-3p, and between miR-330-3p and lncRNA-021545 were investigated in HCCLM3 cells by dual-luciferase reporter assays combined with site mutagenesis. TargetScan (http://www.targetscan.org) and miRDB (http://mirdb.org/miRDB) indicated the CGAAAC sequence of miR-330-3p (**Figure 2A**, **2B**) complementarily binds to GCUUUG sequence at site 3803-3808 of the 3'-UTR of *EREG* (**Figure 2A**) and to GCUUUG sequence at site 1264-1269 of lncRNA021545 (**Figure 2B**). The binding sequence GCUUUG both for EREG and lncRNA-021545 was then mutated to CGAAAC (**Figure 2A**, **2B**).

The luciferase activity was decreased by 29.9% ($P = 0.0142$, **Figure 2A**) in HCCLM3 cells co-transfected with the pmirGlO-*EREG*-3'-UTR-WT luciferase reporter and miR-330-3p mimic, compared with the control group cells co-transfected with pmirGlO-*EREG*-3'-UTR-WT and miR-NC mimic. No luciferase activity change was observed in pmirGlO-*EREG*-3'-UTR-MUT transfected group HCCLM3 cells. In the group cells co-transfected with pmirGlO-lncRNA021545-WT vector and miR-330-3p mimic, the luciferase activity was decreased to 58.9% ($P = 0.0004$, **Figure 2B**) compared with the control group cell. MiR-330-3p mimic transfection had no effect on the luciferase activity of the cells co-transfected with pmirGlO-lncRNA021545-MUT and miR-330-3p mimic (**Figure 2B**). The above results indicated the direct binding of miR-330-3p to *EREG* and lncRNA021545.

MiR-330-3p negatively regulated the expressions of EREG and lncRNA021545. The expression levels of miR-330-3p were upregulated by 21009-($P = 0.0085$) and 15967-folds ($P = 0.0188$) in HuH7 and HCCLM3 cells by its mimic transfections, and downregulated by 96.5% ($P < 0.0001$) and 83.1% ($P < 0.0001$) in HCCLM3 and HuH7 by its inhibitor transfection (**Figure 2C**). Following miR-330-3p overexpression, the endogenous *EREG* and lncRNA-021545 expressions were decreased by 94.3% ($P = 0.0012$) and 45.9% ($P = 0.0007$), EREG protein level was reduced by 57.7% ($P = 0.0009$, **Figure 2D**) in HuH7 cells, and the *EREG* and lncRNA021545 expressions were decreased by 53.5% ($P = 0.0083$) and 40.6% ($P = 0.044$), and EREG protein expression was decreased by 65.0% ($P = 0.0003$, **Figure 2E**) in HCCLM3 cells. Due to miR-330-3p inhibition, the mRNA levels of EREG and lncRNA021545 were increased by 51.4% ($P = 0.0375$) and 79.3% ($P = 0.0012$), and EREG protein expression was increased by 91.2% ($P = 0.0012$, **Figure 2F**) in HuH7 cells, and concordantly, those expression levels of *EREG* mRNA, lncRN-A021545 and EREG protein in HCCLM3 cells were increased by 46.6% ($P = 0.0071$), 52.9% ($P = 0.0029$) and 145.1% ($P = 0.0003$, **Figure 2G**), respectively.

LncRNA021545 downregulation increases miR-330-3p and decreases EREG in HCC cells

We performed siRNA transfection interference to knockdown lncRNA021545 in HCC cells.

Compared with the siRNA NC group cells, the levels of lncRNA021545 were decreased by 60.1% (P = 0.0242) and 66.2% (P = 0.0286, **Figure 2H**) in silncRNA021545 transfected HuH7 and HCCLM3 cells. Following lncRNA-021545 knockdown (**Figure 2H**), the levels of miR-330-3p in HuH7 cells increased by 52.0% (P < 0.0001) and 60.6% (P = 0.0097) in HCCLM3 cells, *EREG* mRNA and EREG protein levels in HuH7 and HCCLM3 cells were decreased by 80.9% (P = 0.0007) and 45.8% (P = 0.0001), and decreased by 31.0% (P = 0.0006) and 33.3% (P = 0.0023), respectively. These results demonstrated that through the direct bindings to miR-330-3p and *EREG*, lncRNA021545 negatively regulated miR-330-3p and positively regulated EREG expression in HCC cells.

EREG alteration on the expressions of miR-330-3p and lncRNA021545 in HCC cells

The expression levels of *EREG* were detected in HuH7 and HCCLM3 cells, and it was found that EREG expression in HCCLM3 cells was 99.9% lower (P = 0.0476, **Figure 2I**) at mRNA level and 71.3% lower at protein level than HuH7 cells, thus, we chose to explore the effect of EREG on the lncRNA021545 and miR-330-3p as well as the metastasis of HCC cells. The expression of EREG was knocked down in HuH7 and overexpressed in HCCLM3 cells. By using siEREG transient transfection interference, EREG was downregulated in siEREG-HuH7 cells by 69.6% (P = 0.0007, **Figure 2J**) at mRNA level and by 39.0% (P = 0.0010, **Figure 2J**) at protein level than those in siNC-HuH7 cells. EREG downregulation led to 34.8% level decrease of lncRNA021545 expression and did not affect the expressions of miR-330-3p in HuH7 cells. Using stable transfection with PCDH-EREG vector by Lentivirus infection through puromycin screening, EREG was upregulated in PCDH-EREG-HCCLM3 cells by 317.1% (P < 0.0001, **Figure 2K**) at mRNA level and by 59.3% (P = 0.032, **Figure 2K**) at protein level than the empty vector transfected PCDH-HCCLM3 cells. EREG overexpression led to 181.1% level increase of lncRNA021545 expression and no change to miR-330-3p expression in HCCLM3 cells.

miR-330-3p influences the in vitro migration and invasion abilities of HCC cells without affecting their proliferation

The influence of miR-330-3p expression on the *in vitro* migration and invasion abilities of HuH7 and HCCLM3 cells were investigated by Boyden transwell chamber assays. MiR-330-3p overexpression promoted the migration and invasion abilities of HCC cells. Compared with HuH7-miR-NC and HCCLM3-miR-NC group cells, the migration and invasion abilities were increased by 66.9% (P = 0.0050) and 70.4% (P = 0.0074, **Figure 3A**) for HuH7-miR-330-3p cells, and increased by 98.9% (P = 0.0008) and 84.9% (P = 0.0037, **Figure 3B**) for HCCLM3-miR-330-3p cells. Accordingly, miR-330-3p downregulation by its inhibitor transfection led to the migration and invasion reductions of 40.4% (P = 0.0001) and 48.0% (P = 0.0003, **Figure 3C**) for HuH7 cells, and of 52.0% (P = 0.0006) and 25.3% (P = 0.0334, **Figure 3D**) for HCCLM3 cells. MTT assay measured miR-330-3p expression on the proliferative capacities of HuH7 and HCCLM3 cells. No apparent changes were determined on the proliferations of HuH7 (**Figure 3E**) and HCCLM3 (**Figure 3F**) cells in responding to either miR-330-3p overexpression or miR-330-3p downregulation. Collectively, miR-330-3p influences the migration and invasion of HCC cells without affecting their proliferations.

EREG affects the in vitro migration and invasion abilities of HCC cells without influencing their proliferation

We further measured the dysexpression of EREG on the migration and invasion abilities of HCC cells. As shown in **Figure 4A**, the numbers of migrated and invaded HCCLM3-PCDH-EREG cells were ~46.7% (P = 0.0005) and ~40.8% (P = 0.0116) of those of HCCLM3-PCDH cells. Consistently, EREG knockdown promoted the migration and invasion abilities of HuH7. The numbers of migrated and invaded HuH7-siEREG cells were 150% (P = 0.0376) and 170% (P = 0.0194, **Figure 4B**) of those of HuH7-siNC cells. EREG decreases the *in vitro* migration and invasion abilities of HCC cells. EREG knockdown by siEREG in HuH7 and overexpression by stable lentivirus PCDH-EREG transfection in HCCLM3 cells did not change the cells' proliferations determined by MTT assays (**Figure 4C**). Our results show EREG plays an important role in the metastatic abilities of HCC cells, while staying uncritical for their proliferations.

lncRNA021545 level negatively correlates with the in vitro migration and invasion of HCC cells

To confirm its tumor inhibitory effect in HCC, we measured the effect of lncRNA021545 knock-

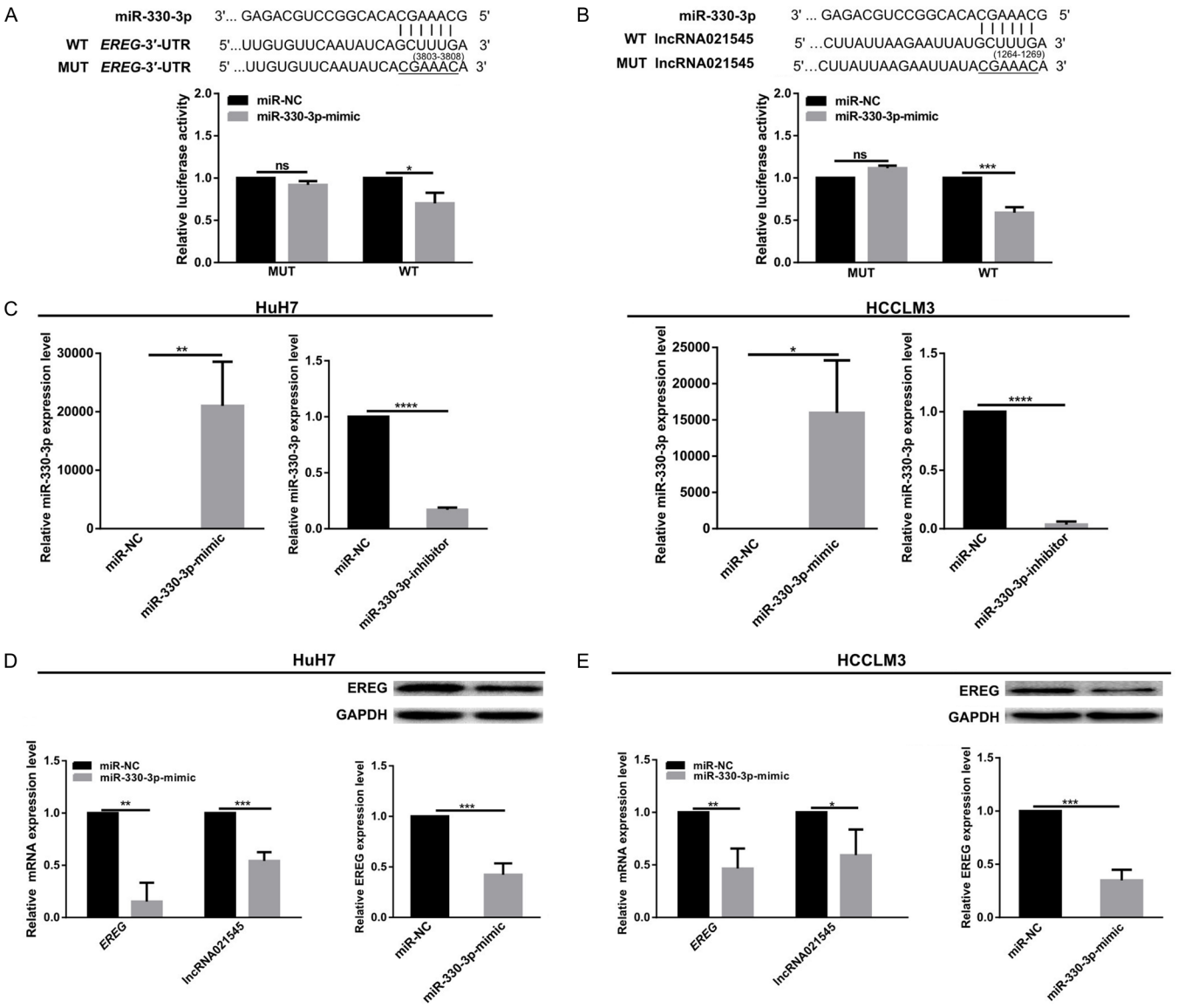
A
miR-330-3p 3'... GAGACGUCCGGCACACGAAACG 5'
WT EREG-3'-UTR 5'...UUGUGUUCAAUAUCAGCUUUGA 3'
(3803-3808)
MUT EREG-3'-UTR 5' ...UUGUGUUCAAUAUCACGAAACA 3'
Relative luciferase activity
miR-NC
miR-330-3p-mimic
ns
*
MUT
WT
B
miR-330-3p 3' ... GAGACGUCCGGCACACGAAACG 5'
WT lncRNA021545 5' …CUUAUUAAGAAUUAUGCUUUGA 3'
(1264-1269)
MUT lncRNA021545 5'…CUUAUUAAGAAUUAUACGAAACA 3'
Relative luciferase activity
miR-NC
miR-330-3p-mimic
ns
***
MUT
WT
C
HuH7
Relative miR-330-3p expression level
**
miR-NC
miR-330-3p-mimic
Relative miR-330-3p expression level
****
miR-NC
miR-330-3p-inhibitor
HCCLM3
Relative miR-330-3p expression level
*
miR-NC
miR-330-3p-mimic
Relative miR-330-3p expression level
****
miR-NC
miR-330-3p-inhibitor
D
HuH7
EREG
GAPDH
Relative mRNA expression level
miR-NC
miR-330-3p-mimic
**
***
EREG
lncRNA021545
Relative EREG expression level
***
miR-NC
miR-330-3p-mimic
E
HCCLM3
EREG
GAPDH
Relative mRNA expression level
miR-NC
miR-330-3p-mimic
**
*
EREG
lncRNA021545
Relative EREG expression level
***
miR-NC
miR-330-3p-mimic

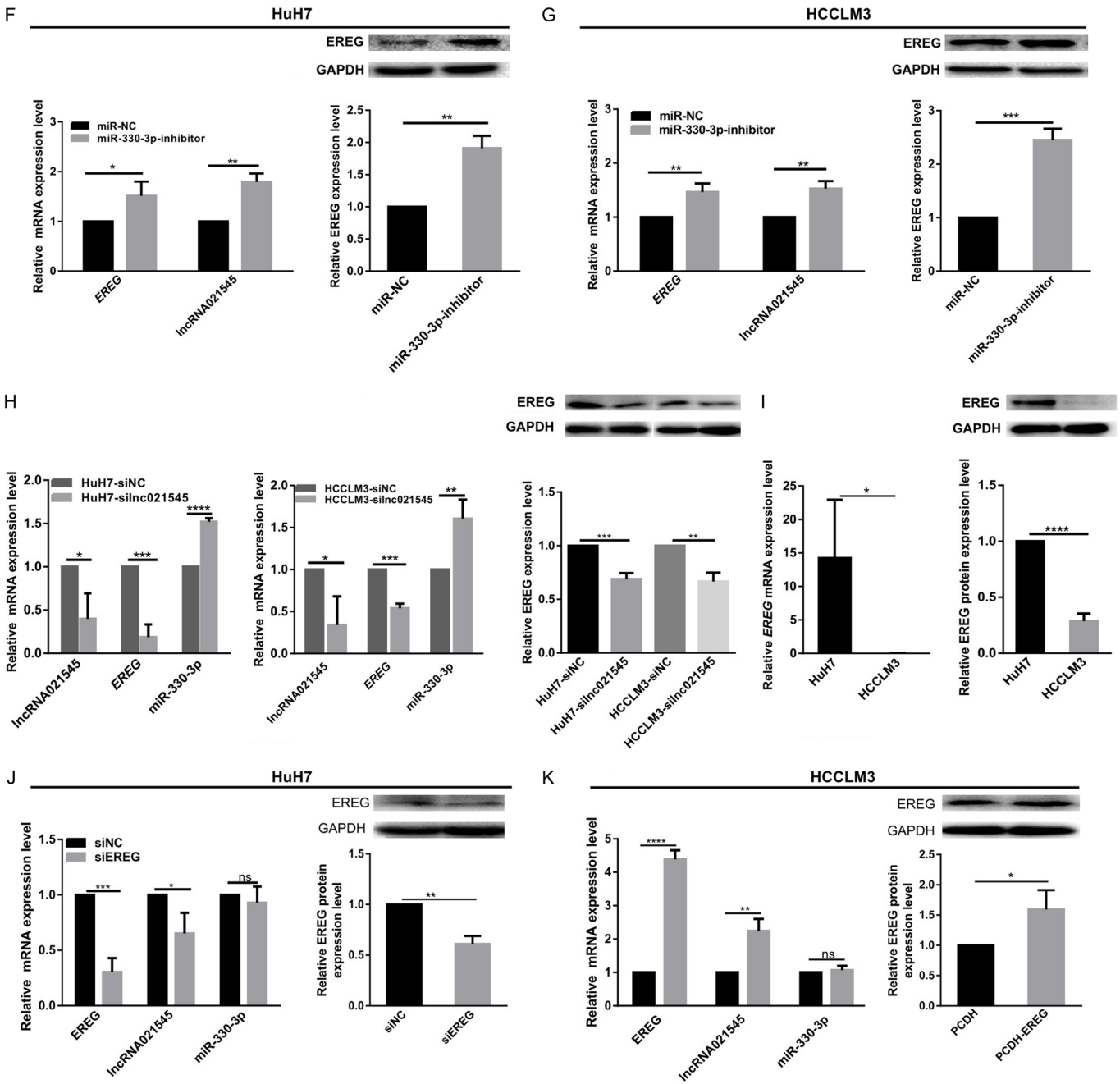
F
HuH7
EREG
GAPDH
miR-NC
miR-330-3p-inhibitor
Relative mRNA expression level
EREG
lncRNA021545
Relative EREG expression level
G
HCCLM3
H
HuH7-siNC
HuH7-silnc021545
HCCLM3-siNC
HCCLM3-silnc021545
miR-330-3p
Relative EREG expression level
I
Relative EREG mRNA expression level
Relative EREG protein expression level
J
siNC
siEREG
ns
Relative EREG protein expression level
K
PCDH
PCDH-EREG

Figure 2. MiR-330-3p directly targets and negatively regulates EREG and lncRNA021545. Bioinformatic prediction of the putative binding sites with the confirmation by mutagenesis-combined to luciferase gene reporting assay for miR-330-3p to *EREG*-3'-UTR. (A) and to lncRNA021545 (B). (C) The overexpression and knockdown of miR-330-3p were performed by its mimic and inhibitor transfections in Huh7 and HCCLM3. The endogenous expressions of EREG and lncRNA021545 were suppressed by overexpressing miR-330-3p in HuH7 (D) and HCCLM3 (E) cells. The endogenous expressions of EREG and lncRNA021545 were promoted by miR-330-3p knockdown in HuH7 (F) and HCCLM3 (G) cells. (H) LncRNA021545 knockdown in HuH7 and HCCLM3 cells resulted in decreased endogenous EREG and increased miR-330-3p expressions. (I) The comparisons of EREG expression at both mRNA and protein levels in HuH7 and HCCLM3 cells. (J) EREG knockdown suppressed lncRNA021545 and showed no effect on miR-330-3p expression in HuH7. (K) EREG overexpression increased lncRNA021545 and showed no change on miR-330-3p expression in HCCLM3 cells.

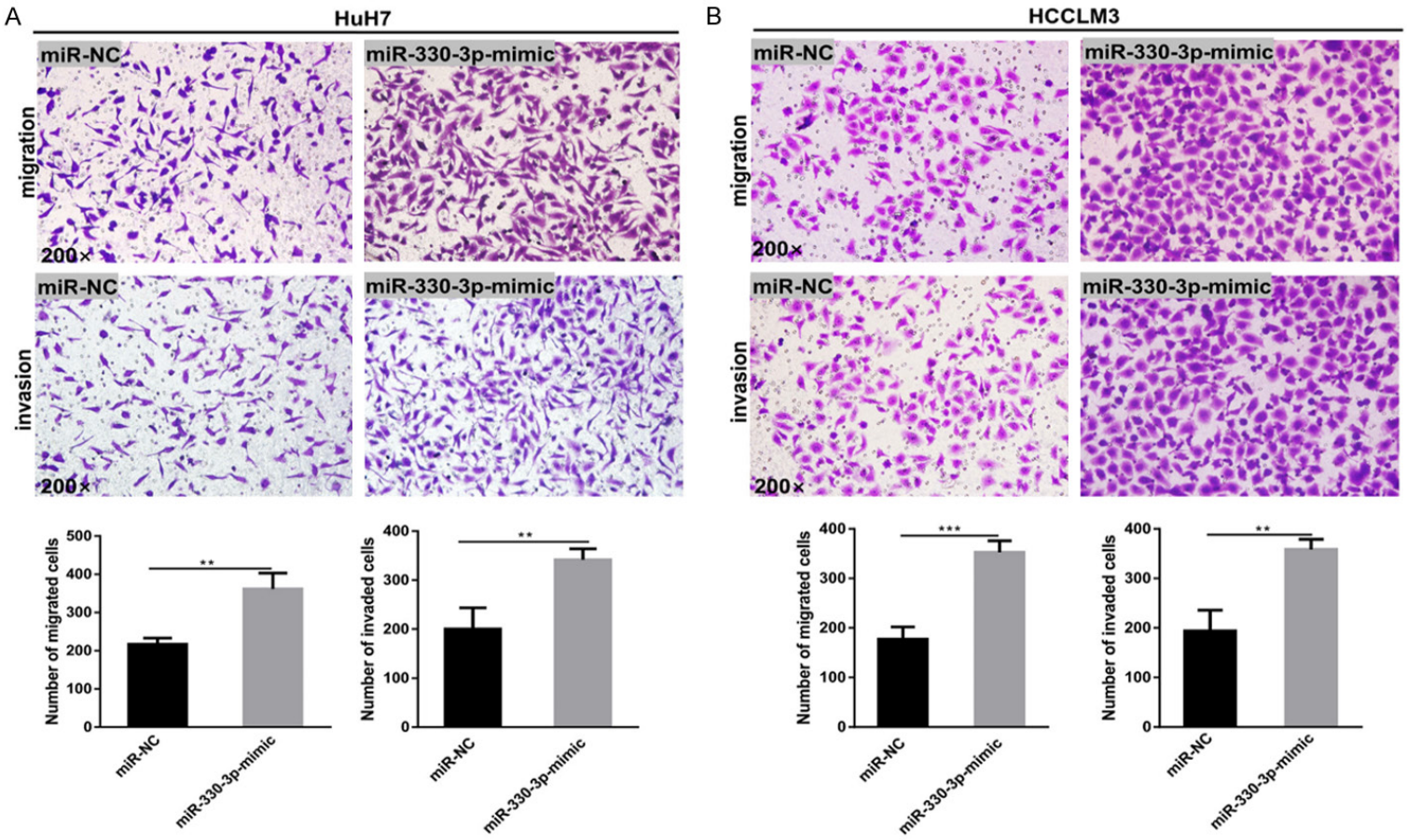

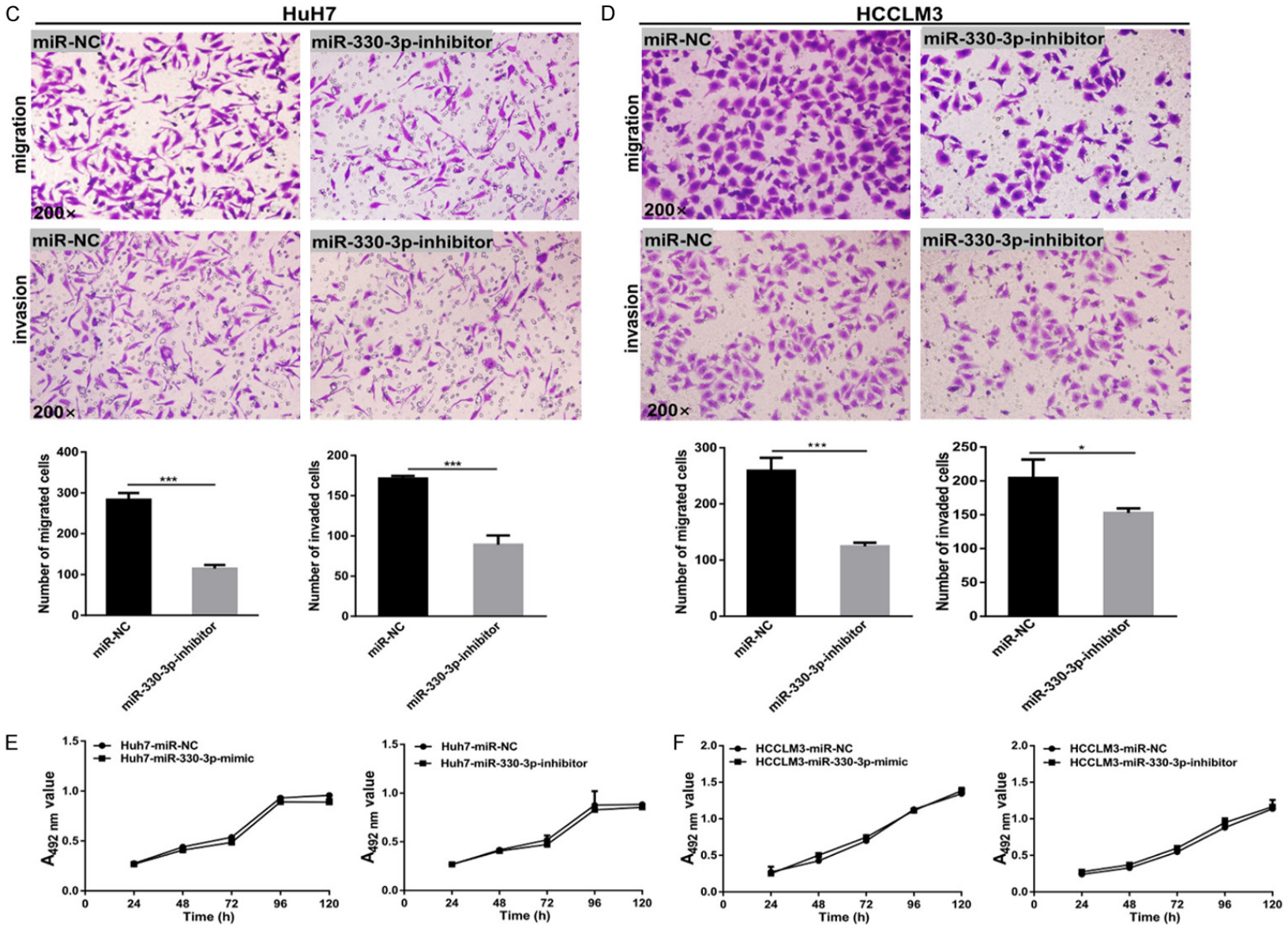

Figure 3. MiR-330-3p dysexpression on the *in vitro* migration, invasion and proliferations of HCC cells. MiR-330-3p overexpression enhanced the migration and invasion abilities of HuH7. (A) and HCCLM3 (B) cells. MiR-330-3p knockdown suppressed the migration and invasion abilities of HuH7 (C) and HCCLM3 (D) cells. MiR-330-3p level change showed no influence on HuH7 (E) and HCCLM3 (F) proliferations by MTT assay.

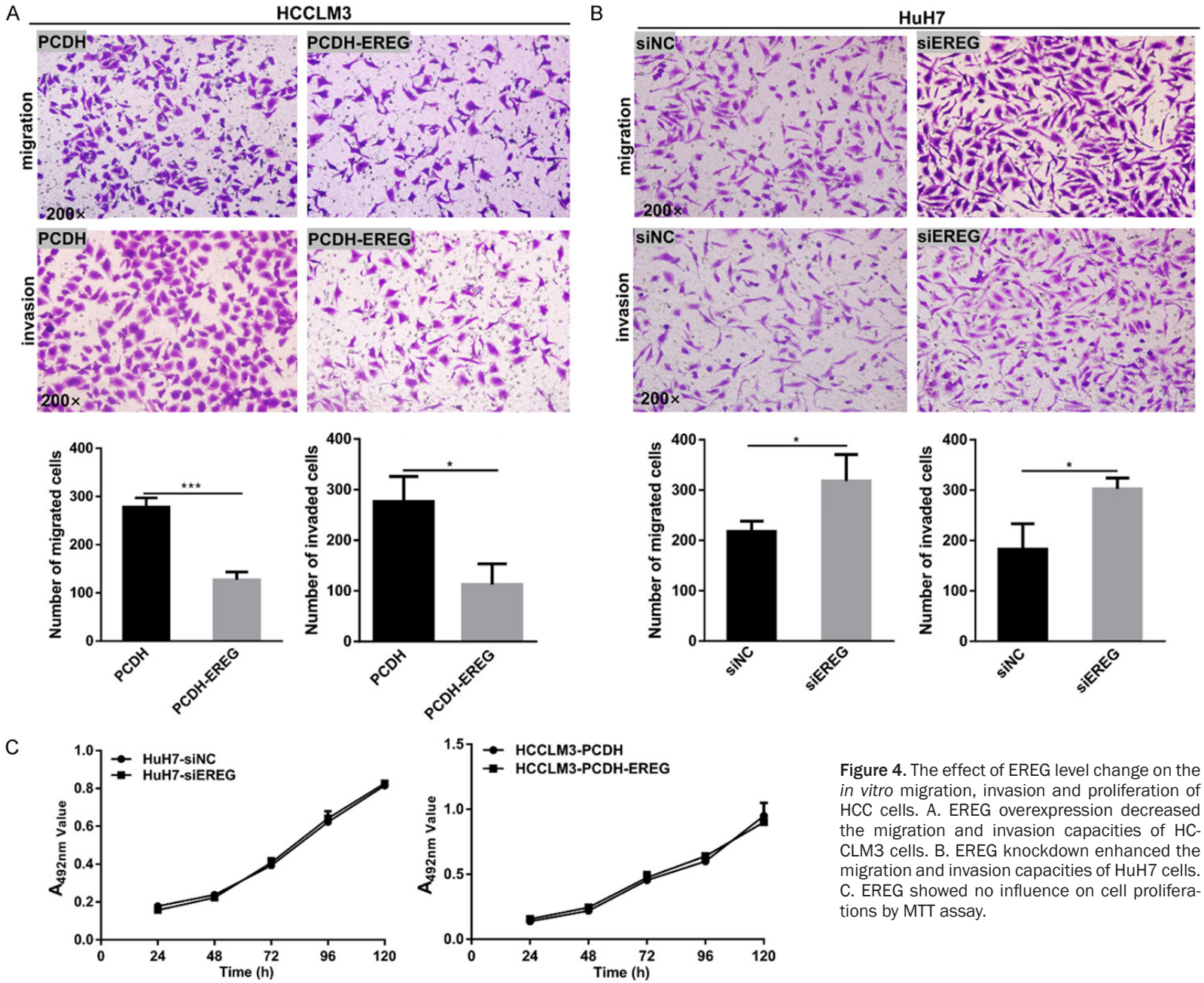

Figure 4. The effect of EREG level change on the *in vitro* migration, invasion and proliferation of HCC cells. A. EREG overexpression decreased the migration and invasion capacities of HCCLM3 cells. B. EREG knockdown enhanced the migration and invasion capacities of HuH7 cells. C. EREG showed no influence on cell proliferations by MTT assay.

down on the migration and invasion capacities of HuH7 and HCCLM3 cells. lncRNA021545 downregulation resulted in their enhanced migration and invasion abilities. The numbers of migrated HuH7-silncRNA021545 and HCCLM3-silncRNA021545 cells increased by 70.9% (P = 0.0003) and 68.5% (P = 0.0020, **Figure 5A**) than those of HuH7-siNC and HCCLM3-siNC cells. The numbers of invaded HuH7-silncRNA021545 and HCCLM3-silncRNA021545 cells increased by 107.2% (P = 0.0044) and 62.7% (P = 0.0042, **Figure 5B**) than those of HuH7-siNC and HCCLM3-siNC cells. The downregulation of lncRNA021545 showed inapparent influence on HuH7 and HCCLM3 proliferations by MTT assays (**Figure 5C**).

miR-330-3p/lncRNA021545/EREG axis mediates the metastasis of HCC cells via EMT

We further explored the miR-330-3p/lncRNA-021545/EREG axial function in HCC malignancy through mediating EMT processes of HuH7 and HCCLM3 cells. Herein, we examined the expression level changes of EMT markers, E-cadherin, N-cadherin, vimentin, snail and slug in both cells following the dysexpressions of EREG, miR-330-3p and lncRNA021545. As in **Figure 6**, knockdown of either EREG or lncRNA021545, and overexpression of miR-330-3p resulted in similar trends on regulating the expressions of the previously mentioned protein molecules, i.e., downregulated epithelial marker E-cadherin and upregulated mesenchymal markers snail, slug, N-cadherin and vimentin in HuH7 and HCCLM3 cells. Consistently, EREG overexpression or miR-330-3p knockdown reduced the expressions of snail, slug, N-cadherin and vimentin, while enhanced E-cadherin expression in HuH7 and HCCLM3 cells.

For EREG, compared with HuH7-siNC cells, EREG knockdown resulted in protein expression increasing of N-cadherin, vimentin, snail and slug with 51.0% (P = 0.0148), 77.7% (P = 0.0339), 46.7% (P = 0.0136), 35.0% (P = 0.0137) and a decrease of E-cadherin protein expression with 41.5% (P < 0.0001, **Figure 6A**) in HuH7-siEREG cells. Compared with HCCLM3-PCDH cells, EREG overexpression decreased the protein expressions of N-cadherin, vimentin, snail and slug by 44.0% (P = 0.0013), 38.7% (P < 0.0001), 38.3% (P < 0.0001), 39.3% (P = 0.0013) and increased E-cadherin protein expression by 33.5% (P = 0.0012, **Figure 6A**) HCCLM3-PCDH-EREG cells. For miR-330-3p, as the results shown in **Figure 6B**, compared with HuH7-miR-NC and HCCLM3-miR-NC group cells, miR-330-3p overexpression upregulated the protein expressions of N-cadherin, vimentin, snail and slug by 71.7% (P = 0.0084) and 96.7% (P = 0.0168), 56.3% (P < 0.0001) and 49.0% (P = 0.0062), 45.0% (P = 0.0024) and 46.0% (P = 0.0048), 59.3% (P = 0.0182) and 57.0% (P = 0.0442) and decreased E-cadherin protein expression by 33.0% (P = 0.0008) and 47.0% (P = 0.0044) in HuH7-miR-330-3p and HCCLM3-miR-330-3p cells. Accordantly, miR-330-3p knockdown decreased the protein levels of N-cadherin, vimentin, snail and slug by 66.0% (P < 0.0001) and 38.7% (P = 0.0130), 31.7% (P = 0.0009) and 33.0% (P = 0.0002), 36.0% (P = 0.0124) and 46.7% (P = 0.0069), 45.7% (P = 0.0388) and 44.3% (P = 0.0446), and increased E-cadherin expression by 41.5% (P < 0.0001) and 63.3% (P = 0.0332) in HuH7 and HCCLM3 cells. For lncRNA021545, as shown in **Figure 6C**, compared with HuH7-siNC and HCCLM3-siNC cells, lncRNA021545 knockdown increased the protein expressions of N-cadherin, vimentin, snail and slug by 58.0% (P = 0.0450) and 72.3% (P = 0.0346), 71.7% (P = 0.0108) and 56.3% (P = 0.0353), 53.0% (P = 0.0198) and 50.3% (P = 0.0005), 47.3% (P = 0.0013) and 55.3% (P = 0.075), and decreased E-cadherin protein expression by 44.0% (P = 0.0009) and 31.0% (P = 0.0034) in HuH7 and HCCLM3 cells.

Is EREG a direct functional mediator of miR-330-3p-effected migration and invasion for HCC cells? Could the *in vitro* phenotypes associated with miR-330-3p deregulation be reversed by opposite EREG expression? We performed a “rescue” experiment by co-transfecting miR-330-3p mimic and PCDH-EREG vector into HCCLM3 cells and the linkages of EMT to miR-330-3p and EREG-mediated tumor migration and invasion were further validated. As shown in **Figure 6D**, miR-330-3p could downregulate endogenous *EREG* mRNA level by 62.2% (P = 0.0311), and protein level by 36.3% (P = 0.0005) in HCCLM3 cells, while, it could only downregulate the EREG expression level in HCCLM3 co-transfected cells with miR-330-3p

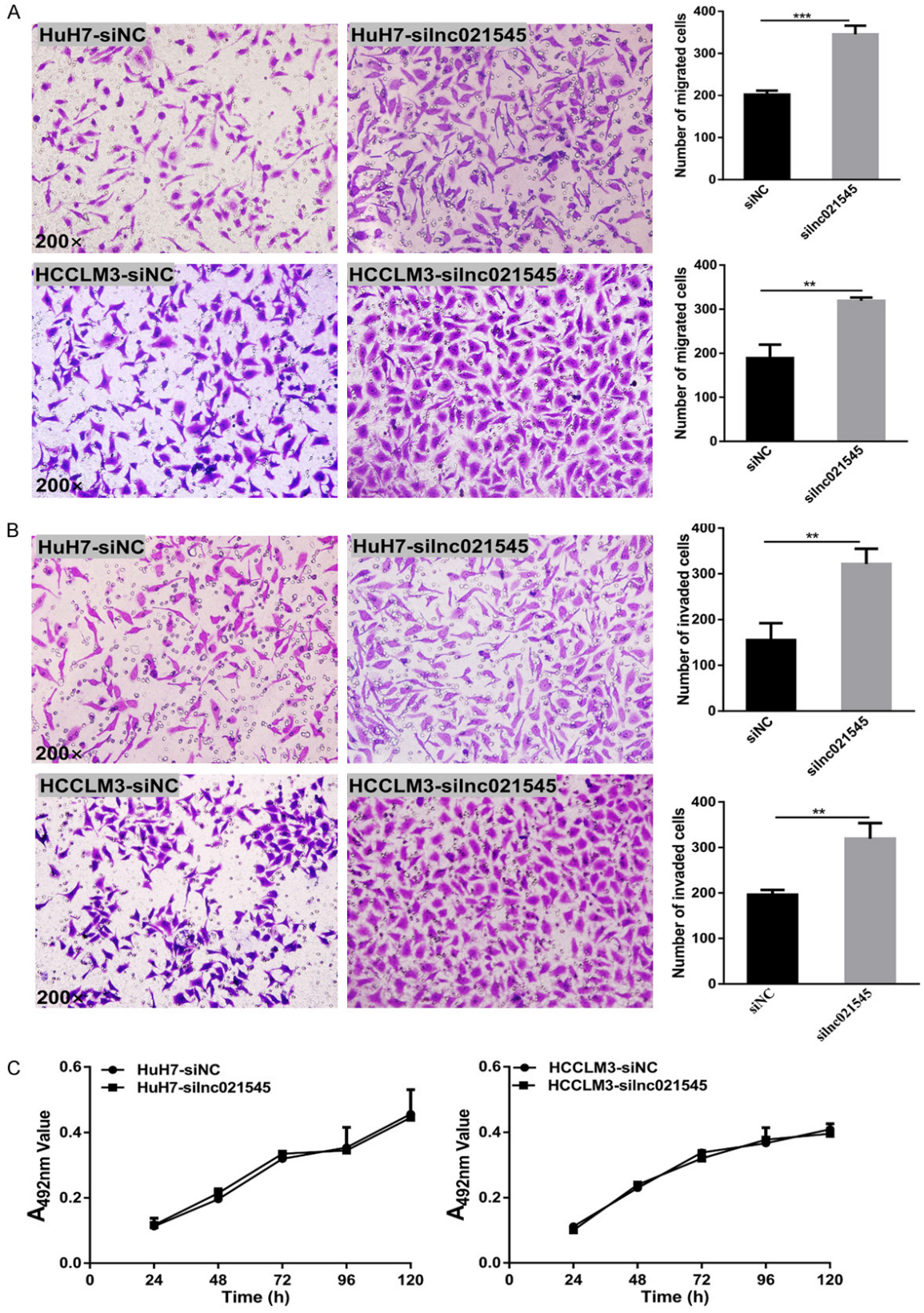

Figure 5. LncRNA021545 knockdown increased the *in vitro* migration and invasion of HCC cells. LncRNA021545 knockdown enhanced migration (A) and invasion (B), and showed no influence on the proliferation (C) capacities of HuH7 and HCCLM3 cells.

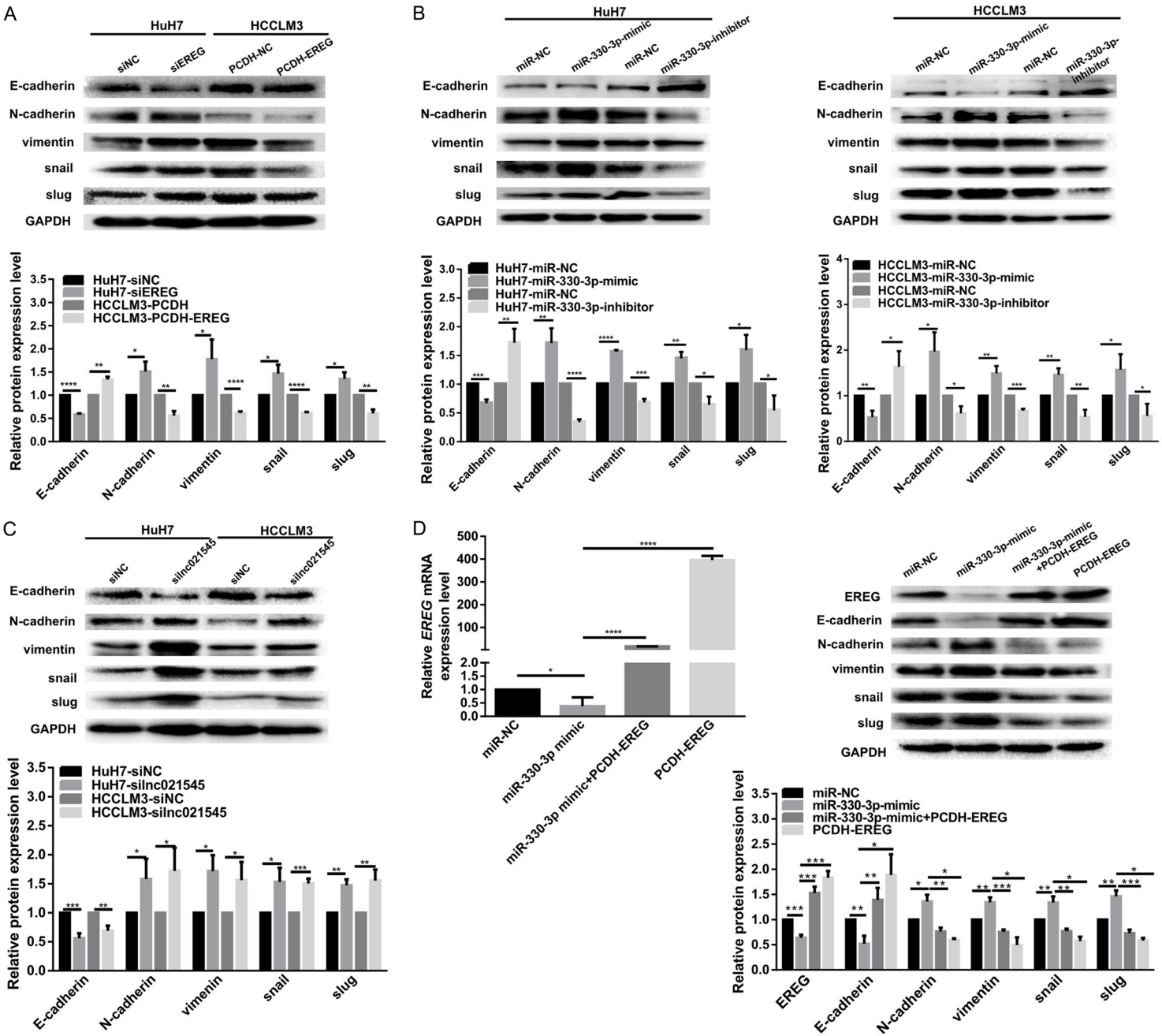
A
HuH7
HCCLM3
siNC
siEREG
PCDH-NC
PCDH-EREG
E-cadherin
N-cadherin
vimentin
snail
slug
GAPDH
Relative protein expression level
HuH7-siNC
HuH7-siEREG
HCCLM3-PCDH
HCCLM3-PCDH-EREG
B
miR-NC
miR-330-3p-mimic
miR-330-3p-inhibitor
HuH7-miR-NC
HuH7-miR-330-3p-mimic
HuH7-miR-330-3p-inhibitor
HCCLM3-miR-NC
HCCLM3-miR-330-3p-mimic
HCCLM3-miR-330-3p-inhibitor
C
siNC
siInc021545
HuH7-siNC
HuH7-siInc021545
HCCLM3-siNC
HCCLM3-siInc021545
D
Relative EREG mRNA expression level
miR-330-3p mimic
miR-330-3p mimic+PCDH-EREG
PCDH-EREG
EREG
miR-330-3p-mimic+PCDH-EREG

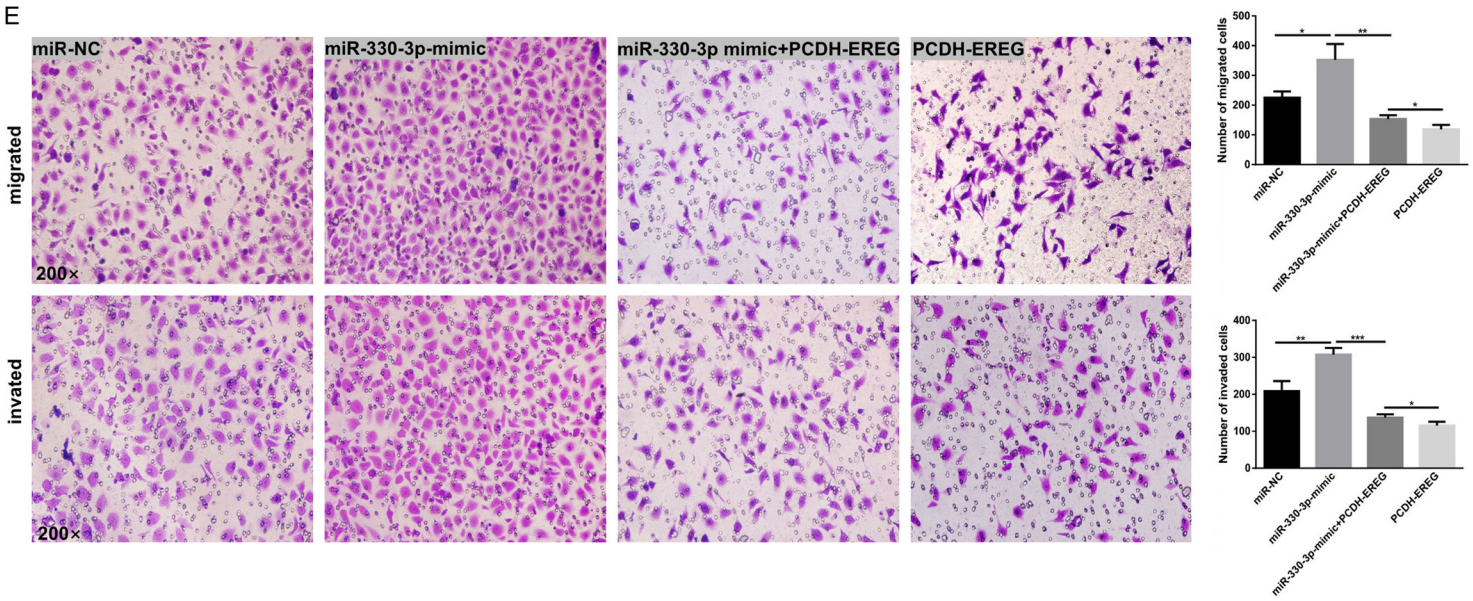

Figure 6. MiR-330-3p/lncRNA021545/EREG axis mediates the metastasis of HCC cells *via* EMT. The influences of EREG (A), miR-330-3p (B) and lncRNA021545 (C) on EMT markers in HuH7 and HCCLM3 cells. The knockdowns of EREG and lncRNA021545 and the overexpression of miR-330-3p increased the protein expressions of N-cadherin, vimentin, snail and slug, and decreased E-cadherin expression. EREG overexpression and miR-330-3p knockdown showed the opposite effects. (D) EREG overexpression by PCDH-EREG transfection reversed the expression changes of E-cadherin, N-cadherin, vimentin, snail and slug induced by miR-330-3p-mimic transfection in HCCLM3 cells. (E) EREG overexpression counteracted the enhanced migration and invasion of HCCLM3 cells in responding to miR-330-3p overexpression.

and PCDH-EREG to certain extent as PCDH-EREG expression vector does not have 3'-UTR domain. Compared with miR-330-3p-mimic group, *EREG* mRNA level was increased by 43.0 fold (P < 0.0001), and protein level was increased by 139.8% (P = 0.0004) in miR-330-3p-mimic+PCDH-EREG group. Meanwhile, the co-transfection of the miR-330-3p mimic and PCDH-EREG resulted in an increased protein expression of E-cadherin by 159.3% (*P* = 0.0031), and suppressed protein expressions of snail, slug, N-cadherin and vimentin by 42.4% (*P* = 0.0017), 50.3% (P = 0.0007), 43.8% (P = 0.0027) and 43.9% (P = 0.0007, **Figure 6D**) compared with the miR-330-3p mimic group. As in **Figure 6E**, exogenous EREG overexpression reversed the positive effect of miR-330-3p on the migration and invasion potentials of HCCLM3 cells. Compared with the HCCLM3-miR-330-3p-mimic group, the migration and invasion abilities of HCCLM3-miR-330-3p+PCDH-EREG cells were reduced by 56.4% (P = 0.003) and 55.4% (P = 0.0001) *in vitro*. The above results proved that miR-330-3p promoted HCC cells migration and invasion by downregulating EREG through binding to *EREG*-3'-UTR, EREG was required for miR-330-3p-mediated HCC cells tumor metastasis.

miR-330-3p promotes the in vivo tumorigenicity and LNM of HCCLM3 cells

To validate in vitro cell line-based studies, we used nude mouse xenograft tumor model to investigate the ectopic expression of miR-330-3p in affecting the *in vivo* tumorigenicity and malignancy of miR-330-3p-mimic-, miR-330-3p-inhibitor- and miR-NC-transfected HCCLM3 cells. As shown in **Figure 7A**, miR-330-3p overexpression by its mimic transfection in HCCLM3 cells contributed in enhanced tumorigenicity speed and tumor mass of xenograft implanted nude mice. miR-330-3p downregulation by its inhibitor in HCCLM3 cells showed no apparent effect on tumor size and mass. Following the subcutaneous injections of three group cells into the right groins of nude mice at the time intervals of 5, 8, 10, 13, 16 and 19 days, the sizes and volumes of the orthotopic transplantation tumors were measured and calculated separately. At 5, 8, 10, 13,16 and 19 (the day when mice were scarified) days, the averaged tumor volumes were 0.0181, 0.0192, 0.0298, 0.0388, 0.0447 and 0.0517 mm^3 for miR-NC, 0.0173, 0.0218, 0.0378, 0.0590, 0.0697 and 0.0863 mm^3 for HCCLM3-miR-330-3p-mimic and 0.0163, 0.0188, 0.0351, 0.0430, 0.0435 and 0.0467 mm^3 for HCCLM3-miR-330-3p-inhibitor group mice. No apparent tumor volume difference was observed between HCCLM3-miR-330-3p-inhibitor and -miR-NC group mice. While, compared with the above two group mice, the tumor volumes of HCCLM3-miR-330-3p-mimic group mice were bigger at different time intervals and showed apparent increases of 52.1% (P = 0.0460), 55.9% (P = 0.0457) and 66.9% (P = 0.0051, **Figure 7A**) on day 13, 16 and 19, respectively. The tumor masses dissected from HCCLM3-miR-NC, -miR-330-3p-mimic and -miR-330-3p-inhibitor group mice were weighted with the averages of 0.0342, 0.0849 and 0.0363 g (**Figure 7A**). The primary tumor mass of HCCLM3-miR-330-3p-mimic group showed a 148.2% (P = 0.0358, **Figure 7A**) increase than HCCLM3-miR-NC mice. Consistently, no tumor mass difference was observed for HCCLM3-miR-330-3p-inhibitor group mice than the control.

The level change of miR-330-3p on the lymphatic metastases of HCCLM3 cells to inguinal, pararenal and axillary LNs was investigated. On the 19th day following the transplantations of tumor cells into nude mice, as shown in **Figure 7B**, the averaged masses of dissected inguinal, pararenal and axillary LNs from HCCLM3-miR-330-3p-mimic group mice were measured with the increased of 44.4% (P = 0.0055), 46.9% (P = 0.0231) and 76.1% (P = 0.0093), while, from HCCLM3-miR-330-3p-inhibitor group mice were measured with the decreased of 32.1% (P = 0.0489), 41.1% (P = 0.0494) and 70.9% (P = 0.0314) than those from HCCLM3-miR-NC mice. We further examined miR-330-3p's effect on the morphologies of LNs by HE staining assay. For inguinal and pararenal LNs from HCCLM3-miR-NC- and HCCLM3-miR-330-3p-inhibitor group mice, their structures were still distinct without obvious pathological changes, the cell morphology was regular, the cells were arranged more neatly and tightly, and the cell nuclei were stained clear and deep (**Figure 7C**). For HCCLM3-miR-330-3p-mimic group mice, the metastatic foci, cell clusters composed of numerous tumor cells, appeared in marginal sinus of inguinal and pararenal LNs sections. Among them, indi-

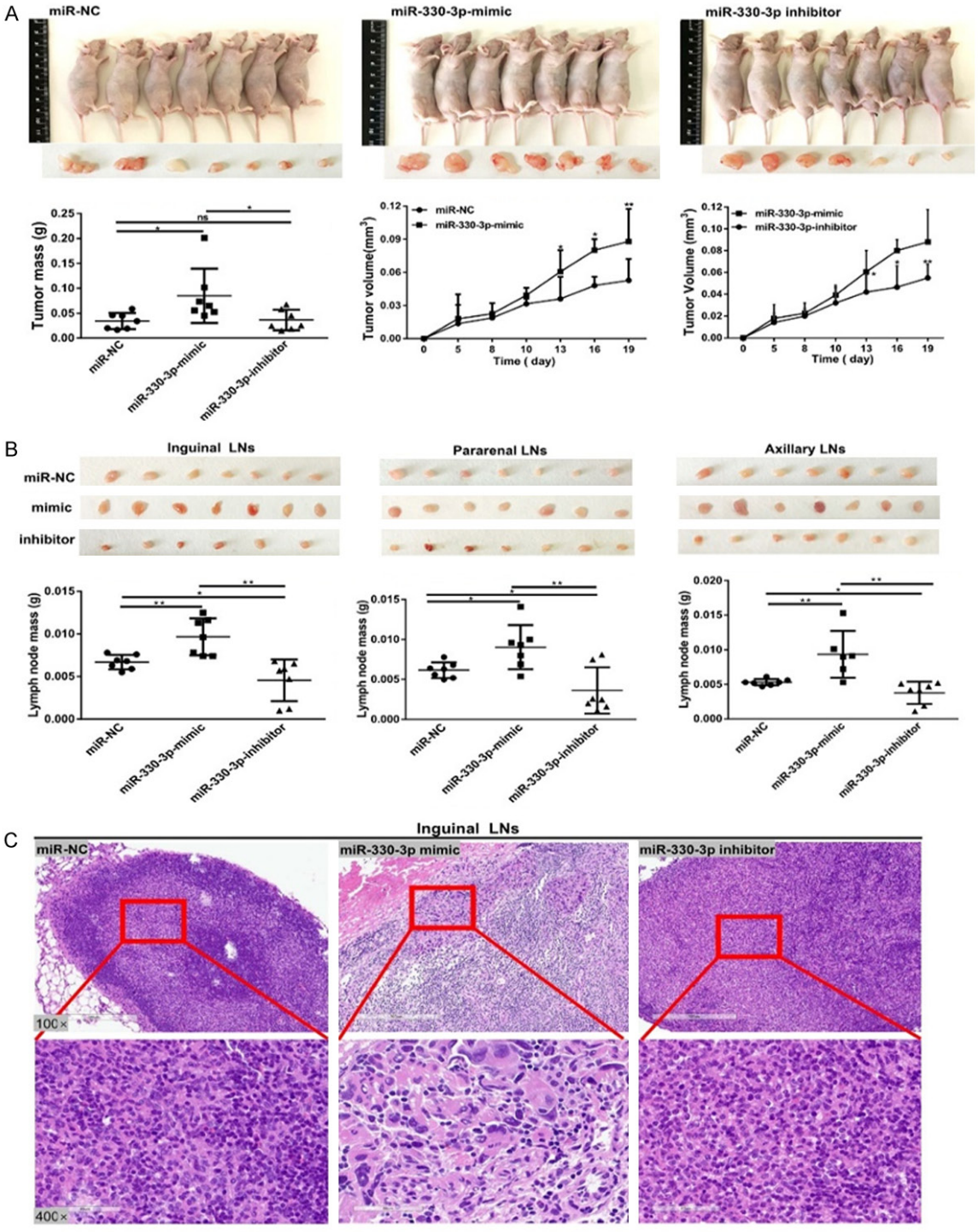
A
miR-NC
miR-330-3p-mimic
miR-330-3p inhibitor
Tumor mass (g)
Tumor volume(mm3)
Tumor Volume (mm3)
Time (day)
B
Inguinal LNs
Pararenal LNs
Axillary LNs
miR-NC
mimic
inhibitor
Lymph node mass (g)
C
Inguinal LNs
miR-330-3p mimic
100×
400×

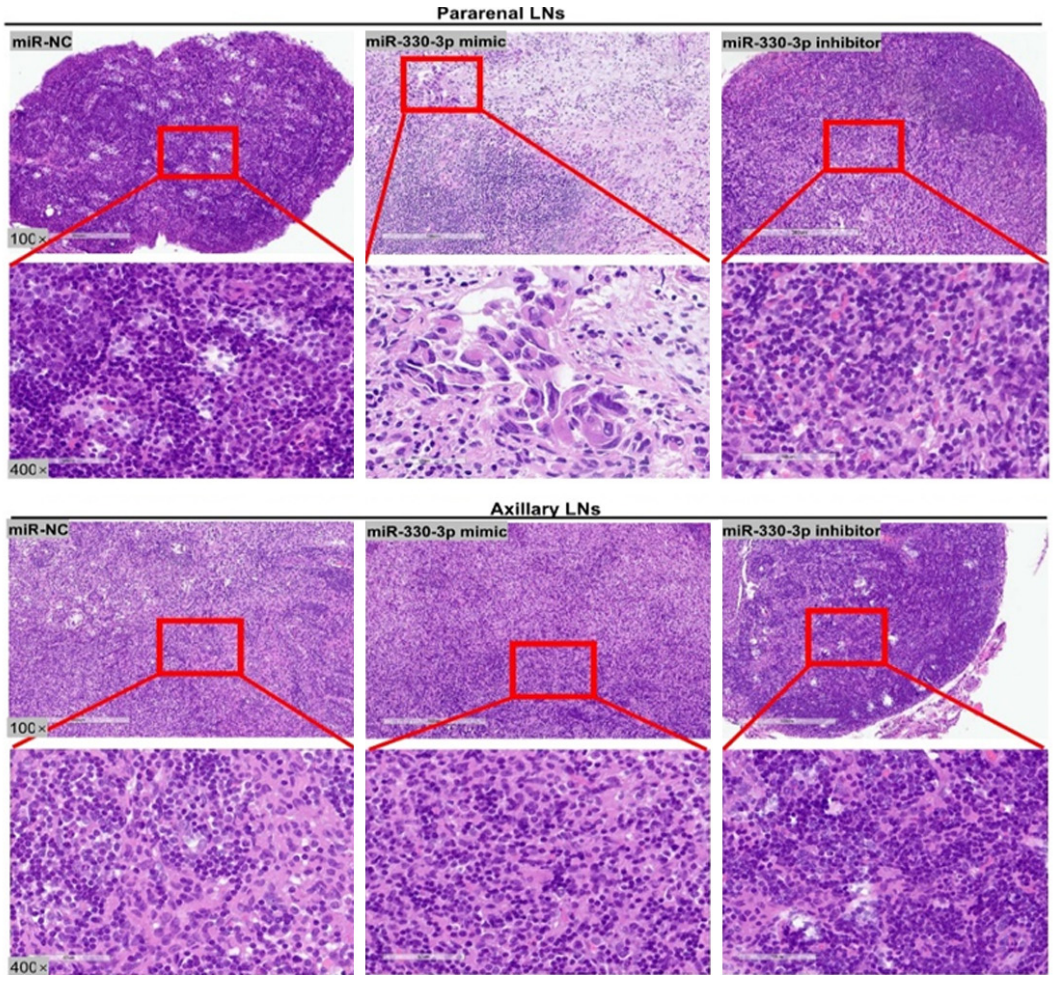

Figure 7. MiR-330-3p promotes the *in vivo* tumorigenicity and metastasis of HCCLM3 cells. A. The effect of miR-330-3p overexpression and knockdown on the *in vivo* tumorigenesis of HCCLM3 cells. MiR-330-3p overexpression by mimic transfection promoted the *in vivo* tumor forming speed and size for HCCLM3-miR-330-3p-mimic transplanted nude mice. miR-330-3p knockdown by its inhibitor transfection showed unapparent effect on HCCLM3 tumorigenesis in nude mice. B. Overall, miR-330-3p overexpression increased and miR-330-3p knockdown decreased the lymph node metastasis of HCCLM3 cells. Compared with HCCLM3-miR-NC group mice, the inguinal, pararenal and axillary LNs dissected from HCCLM3-miR-330-3p-mimic and HCCLM3-miR-330-3p-inhibitor transplanted mice showed increased and decreased masses, respectively. C. HE staining assays of inguinal, pararenal and axillary LNs. Metastatic foci, intercellular heteromorphism and inflammation were clearly obtained in the marginal sinus of inguinal and pararenal LNs from HCCLM3-miR-330-3p-mimic transplanted mice although without unapparent morphology changes observed in axillary ones. For HCCLM3-miR-NC- and HCCLM3-miR-330-3p-inhibitor mice, the structures of inguinal, pararenal and axillary LNs were distinct and intact.

vidual cells were polygonal in shape, disorderly arranged in size, and distributed in a sheet with obscure boundary for cytoplasm, increasing nuclear/plasma ratio and clear intercellular heteromorphism. The tumor cells adhered obviously with notable sinus infiltration and clear boundaries against normal lymphoid tissues. Following inflammatory response, small lymphocytes appeared among tumor cells, and some of them were surrounded by lymphoid follicles with expanded interfollicular area and enriched blood vessels (**Figure 7C**). No apparent morphology changes were observed for the axillary LNs among HCCLM3-miR-NC, HCCLM3-miR-330-3p-mimic and HCCLM3-miR-330-3p-inhibitor group mice (**Figure 7C**), which might be due to the short infection duration in which the proximal LNs rather than the distant LNs of the tumor cell bearing mice showed lesions. These results indicated that miR-330-3p upregulation promoted the *in vivo* LNM potential of HCCLM3 cells.

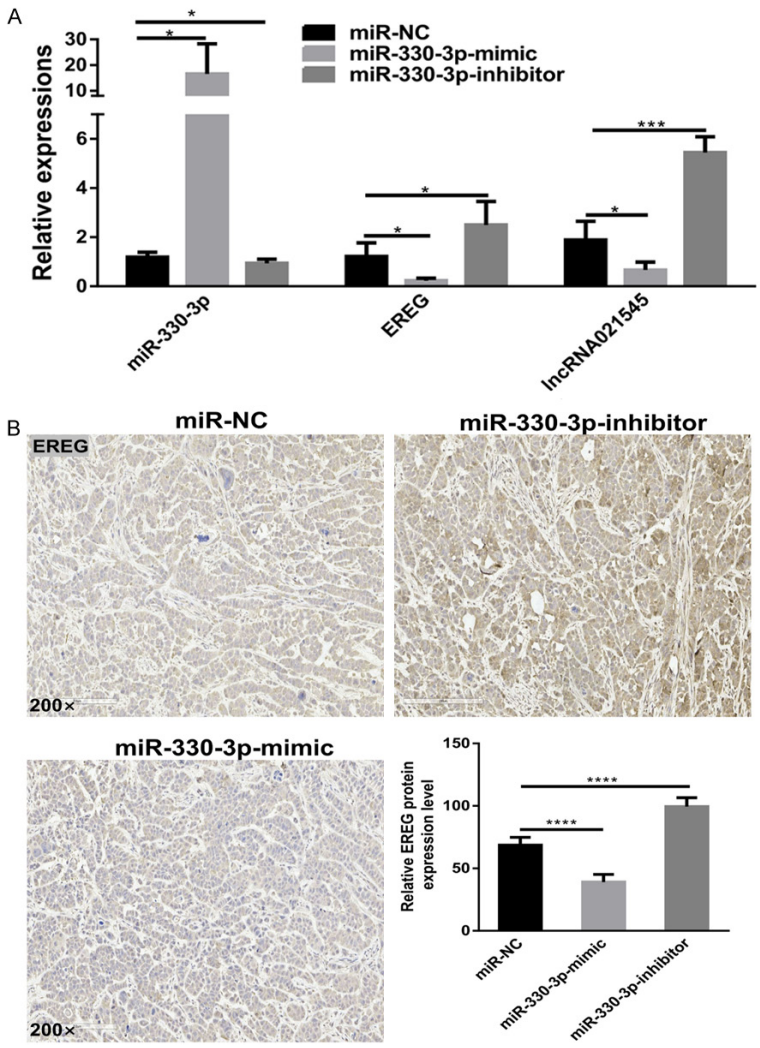

Figure 8. MiR-330-3p dysexpression negatively correlates with EREG and lncRNA021545 in primary tumors of HCCLM3 bearing nude mice. A. Compared with HCCLM3-miR-NC group mice, qRT-PCR assay showed that miR-330-3p was upregulated and both EREG and lncRN021545 were downregulated in primary tumors from HCCLM3-miR-330-3p-mimic group mice, while, miR-330-3p was downregulated and both *EREG* and lncRN021545 were upregulated in primary tumors from HCCLM3-miR-330-3p-inhibitor group mice. B. Compared with HCCLM3-miR-NC mice, IHC showed EREG expression was downregulated and upregulated in primary tumors from HCCLM3-miR-330-3p-mimic and HCCLM3-miR-330-3p-inhibitor transplanted mice, respectively.

miR-330-3p upregulation negatively regulates EREG and lncRNA021545 in nude mice orthotopic transplantation tumors

As shown in **Figure 8A**, miR-330-3p expression level in nude mice orthotopic transplantation tumors was negatively correlated with the levels of lncRNA021545 and EREG. Compared with HCCLM3-miR-NC bearing group mice, qRT-PCR results showed the lncRNA021545 and EREG expression levels in primary tumor tissues decreased by 65.7% (P = 0.0465) and 81.4% (P = 0.0249) from HCCLM3-miR-330-3p-mimic bearing group mice, and increased by 188.1% (P = 0.0001) and 105.8% (P = 0.0383) from HCCLM3-miR-330-3p-inhibitor bearing group mice, respectively. Consistently, IHC assay (**Figure 8B**) indicated that miR-330-3p upregulation and downregulation led to a 42.9% (P < 0.0001) reduction and a 45.1% (P < 0.0001) increase of EREG protein expression in primary tumors obtained from HCCLM3-miR-330-3p-mimic and -inhibitor group mice, respectively.

The influence of miR-330-3p dysexpression on critical EMT molecules in nude mice orthotopic transplantation tumors

We further examined the expressions of EMT protein markers in the primary tumors from the three group tumor cells implanted nude mice by IHC assay. As the results shown in **Figure 9A**, compared with the HCCLM3-miR-NC group mice, the expression levels of snail, slug, N-cadherin and vimentin increased by 43.0% (P < 0.0001), 44.9% (P = 0.0002), 31.5% (P < 0.0001) and 30.2% (P = 0.0019), E-cadherin decreased by 82.8% (P < 0.0001) in primary tumors from HCCLM3-miR-330-3p-mimic mice, while, the levels of snail, slug, N-cadherin and vimentin decreased by 42.9% (P < 0.0001), 37.5% (P = 0.0009), 52.9% (P < 0.0001) and 37.0% (P = 0.0002) E-cadherin expression increased by 101.4% (P < 0.0001) for HCCLM3-miR-330-3p-inhibitor mice.

Consistent with the *in vitro* cellular experiment results, IHC indicated that miR-330-3p dysex-

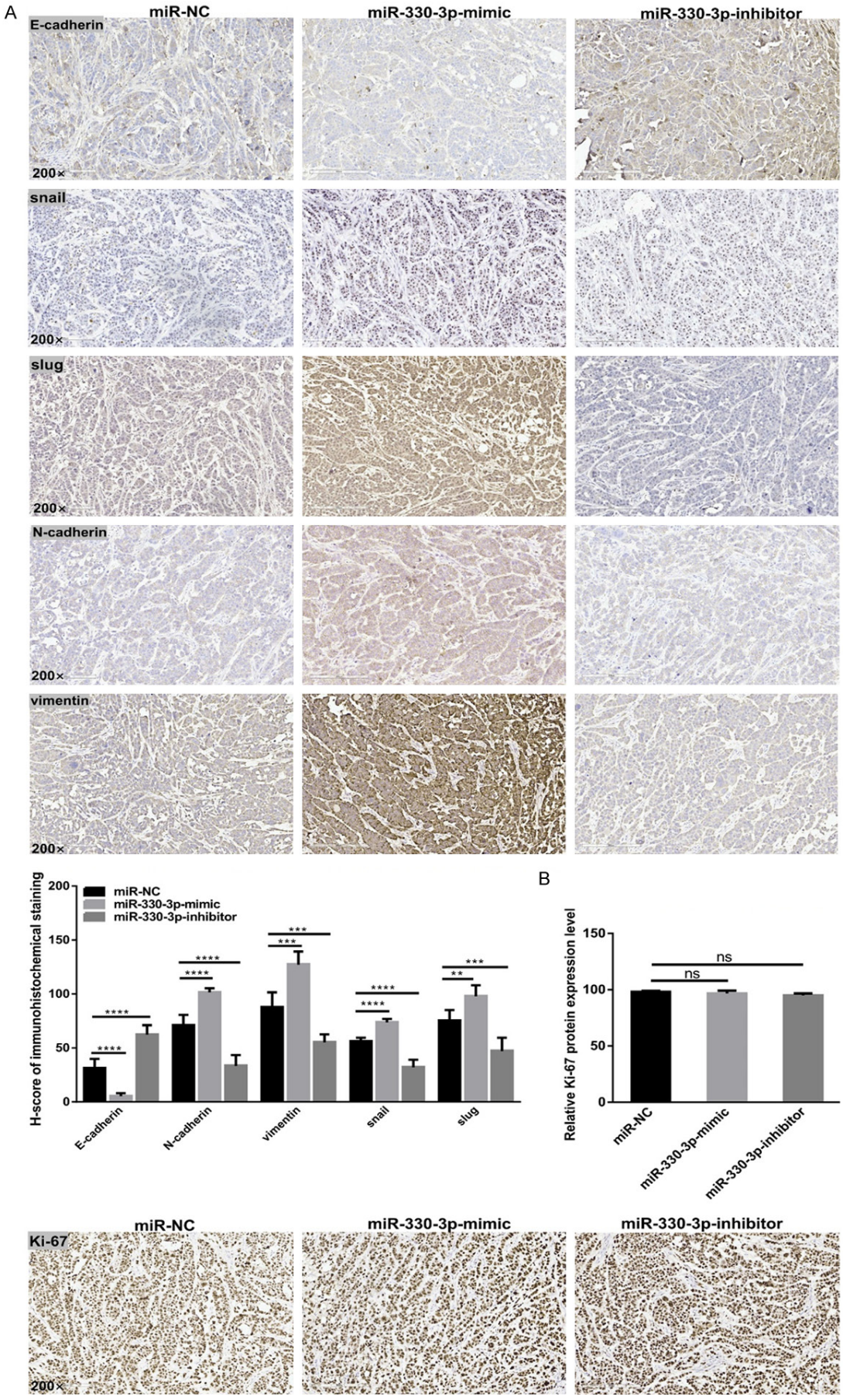
A
miR-NC
miR-330-3p-mimic
miR-330-3p-inhibitor
E-cadherin
snail
slug
N-cadherin
vimentin
Ki-67
200×
H-score of immunohistochemical staining
miR-NC
miR-330-3p-mimic
miR-330-3p-inhibitor
E-cadherin
N-cadherin
vimentin
snail
slug
B
Relative Ki-67 protein expression level
ns
miR-NC
miR-330-3p-mimic
miR-330-3p-inhibitor

Figure 9. The influence of miR-330-3p dysexpression on key EMT related molecules in primary tumors of HCCLM3 bearing nude mice. A. Compared with HCCLM3-miR-NC group mice, IHC assays showed the decrease of E-cadherin and the increases of N-cadherin, vimentin, slug and snail in HCCLM3-miR-330-3p-mimic transplanted mice, and consistently the increase of E-cadherin and the decreases of N-cadherin, vimentin, slug and snail in HCCLM3-miR-330-3p-inhibitor mice. B. IHC assay showed no apparent expression change of Ki-67 in primary tumors among HCCLM3-miR-330-3p-mimic, -inhibitor and -miR-NC group mice.

pression probably showed no influence on HCCLM3 cell proliferation in orthotopic transplantation tumors in nude mice. Compared with the HCCLM3-miR-NC group mice, Ki-67 expressions in primary tumors obtained either from HCCLM3-miR-330-3p-mimic mice or HCCLM3-miR-330-3p-inhibitor group mice had no apparent changes (**Figure 9B**). The results showed miR-330-3p could promote metastasis of HCC cells by regulating EMT markers, but showed no effect on *in vivo* proliferation of HCCLM3 cells.

Discussion

Liver cancer ranks as the fifth most common cancer malignancies and the second largest cancer-related deaths worldwide [1]. Hepatocellular carcinoma (HCC) is a primary liver malignancy accounting for 85-90% of liver cancer [53]. Hepatectomy and liver transplantation provide a curative opportunity for the patients diagnosed without metastasis with a 5-year survival rate of 50-70% [54]. However, the prognosis of HCC is still poor due to tumor metastases result in its recurrence rate over 50% at 5 years [55].

Epithelial-mesenchymal transition (EMT) process plays an important role in cancer invasiveness. The loss of epithelial-like characteristics and the gain of mesenchymal-like attributes promote the migration and invasion of tumor cells in cancer development and metastasis including HCC [2, 56]. Its hijack by cancer cells lead to the latters' morphological changes from cobblestone-like epithelial cells with an apical basal polarity to dispersed, spindle-shaped mesenchymal cells with migratory protrusions [57], which then promote the invasion and spread cancer cells throughout the organism. The effectors including cadherins, fibronectin, vimentin and integrins as well as transcription factors including snail, slug, Twist and Zeb for EMT are well-known and -investigated in cancer carcinogenesis and malignancy [2, 5]. Expressions of these markers are regarded as a harbinger of the onset of EMT, an indicator of the cancer metastasis and important targeting indicators of the chemotherapy and small molecule targeted therapies of cancers [58, 59]. The study on novel molecular action mechanisms, particularly the upstream regulation molecules together with their functional mechanism to trigger HCC malignancy through EMT process are critical to benefit its prevention, diagnosis and treatment. This study revealed a new competitive endogenous RNA (ceRNA) mechanism in hepatocarcinoma. The results suggest that microRNA-330-3p (miR-330-3p) binds to long non-coding RNA 021545 (lncRNA-021545) and 3'-UTR of epiregulin (EREG) to negatively regulate their expressions *in vitro* and *in vivo*, moreover, lncRNA021545 inhibits miR-330-3p expression through ceRNA regulation, then indirectly positively regulates the expression of EREG. Herein, we investigated a novel miR-330-3p/lncRNA021545/EREG signaling regulation of hepatocarcinoma malignancy *via* EMT process.

MiR-330-3p has been reported to act as a tumor promotion or suppression factor in carcinogenesis depending on cancer types. Its upregulation was linked to glioma [15], lung cancer [17], esophageal squamous cell carcinoma [18], liver cancer [20], breast [19, 60], pancreatic [21], and ovarian [61] cancers. MiR-330-3p overexpression enhanced the *in vitro* migration and invasion capacities of the cell lines of breast cancer [19], lung cancer [17] and esophageal squamous cell carcinoma [18]. Higher miR-330-3p expressions was associated with lower survival rate and poor prognosis of breast cancer and ovarian cancer patients [19, 60, 61]. While, the downregulation of miR-330-3p was related to the development and progressions of osteosarcoma [23], gastric cancer [24], bladder cancer [25], tongue squamous cell carcinoma [62], glioma [63] and colorectal cancer [26]. Downregulation of miR-330-3p in glioma [63] and colorectal cancer [26] cell lines resulted in their suppressed *in vitro* migration and invasion. Interestingly, even in the same type of cancer like glioma, miR-330-3p was paradoxically reported as a promoter [15] and as a suppresser [63] by sepa-

rate investigators, which reflects the complexity of the molecular functional mechanism of liver cancer.

Two separate group works showed the involvement of miR-330-3p in liver cancer [20, 29]. Probably due to the control specimens used, miR-330-3p was measured upregulated in 30 HCC tumorous tissues compared with that in paracancerous tissues [20], and the other study showed a downregulation of miR-330-3p in 30 liver cancer tissues compared with 20 normal tissues [29], however, the source and the definition of "normal" tissues were not mentioned in the study. MiR-330-3p affected the *in vitro* migration and invasion capacities of HCCLM3 cells via targeting BTG1 [20] and HepG2 via targeting MAP2K1 [29]. Herein, we strictly performed one-to-one detection of miR-330-3p expression between the tumorous and paired paracancerous non-tumor tissues from individual patient and statistically summarized its expression difference. Current work indicated that miR-330-3p was upregulated (**Figure 1B**) in 26 HCC patients' tumorous tissues. Thus, current work demonstrates the upregulation of miR-330-3p was potentially involved in promoting HCC malignancy. Meanwhile, we found EREG mRNA and protein (**Figure 1A**) and lncRNA021545 (**Figure 1B**) were downregulated in HCC patients' tumorous tissues, which suggested they probably acted as suppressing factors in HCC malignancy. More important and exciting was their deficiencies with apparent positive correlation (**Figure 1F**) in HCC tumorous tissues inversely correlated with miR-330-3p overexpression (**Figure 1D**, **1E**). The evidences provided us with the clues to the indu-vial important roles of these three molecules together with the definitive mutual regulations in liver cancer.

Epiregulin (EREG) is a member of the epidermal growth factor (EGF) family, located on chromosome 4q13.3. EREG exhibits dual functions in different cancers. It was reported overexpressed in head and neck squamous cell carcinoma [39] and downregulated in colorectal and rectal cancers [48]. Higher EREG expression level predicted a clear longer overall survival for patients with rectal [47], colorectal [48, 64], and neck squamous cell [65] cancers. EREG plays important roles in hepatic injurie [66] and in liver regeneration [67]. However, the expression profile, the influence on malignancy with its molecular regulation mechanism of EREG in HCC are poorly understood. In current work, we demonstrated that EREG decreased in tumorous tissues and functioned together with miR-330-3p and lncRNA021545 in HCC malignancy. LncRNA021545 (NONCODE ID: NONHSAT021545.2) is a 3149-bp long chain non-coding RNA located on chromosome 11. Only one publication is available so far mentioning its potential involvement in human schizophrenic [38] without further in-depth research. In short, the role and action mechanism of lncRNA021545 in almost all areas have been untouched yet. In this work, we linked lncRNA021545 deficiency (**Figure 1C**) with the dysexpressions of miR-330-3p and EREG to the clinical progression and malignancy of HCC.

The above evidences demonstrated the dysregulations of EREG, miR-330-3p and lncRNA-021545 as well as their potential crosstalks in HCC malignancy. We first established their association through a novel ceRNA regulation mechanism in HCC. Bioinformatic analyses predicted the possible direct bindings of the CGAAAC site of miR-330-3p (**Figure 2A**, **2B**) to the GCUUUG site at 3803-3808 of *EREG*'s 3'-UTR (**Figure 2A**) and to the GCUUUG site (1264-1269) of lncRNA021545 (**Figure 2B**). Dual luciferase reporter gene assay combined to mutagenesis PCR confirmed the direct binging of miR-330-3p EREG and lncRNA021545 (**Figure 2A**, **2B**). Consequently, miR-330-3p overexpression negatively regulated EREG and lncRNA021545 expression levels (**Figure 2D**, **2E**) in HuH7 and HCCLM3 cells, vice versa (**Figure 2F**, **2G**). EREG showed no influence on miR-330-3p in HCC cells. Neither the overexpression nor the knockdown of EREG changed the expression levels of miR-330-3p in HCCLM3 and HuH7 cells (**Figure 2J**, **2K**). EREG positively mediated lncRNA021545 expression in cells. Its overexpression or knockdown accordingly increased or decreased the expression levels of lncRNA021545 in HCCLM3 and HuH7 cells (**Figure 2J**, **2K**). In ceRNA hypothetical regulation mechanism, lncRNAs act as endogenous decoys for miRNAs to further hinder the latters' binding with targeting mRNAs [68-70] for their expressions and play important roles in human cancers. Although we failed to overexpress lncRNA021545 in HuH7 and HCCLM3 cells, our experiment results clearly showed the knockdown of lncRNA021545

resulted in apparent increased expression of miR-330-3p and decreased expression of EREG in them (**Figure 2H**). Therefore, the results from current work on the direct bindings among miR-330-3p, EREG and lincRNA021545 with their mutual regulation correlationships in hepatocarcinoma cells and dysexpression correlations in tumorous tissues of hepatocarcinoma patients demonstrate a novel ceRNA regulatory mechanism in hepatocarcinoma malignancy. To our knowledge, the function and mechanism of this pathway has not been reported yet so far in human disease.

We further found that miR-330-3p/lncRNA-021545/EREG axis influences the migration and invasion rather than proliferation abilities of HCCLM3 and Huh7 cells. Neither the overexpression and knockdown of miR-330-3p, nor the overexpression and knockdown of EREG, nor the knockdown of lncRNA021545 changed the proliferation abilities of HCCLM3 and HuH7 cells by MTT assay (**Figures 3E**, **3F**, **4C** and **5C**). While, the migration and invasion behaviours of HCCLM3 and HuH7 are enhanced due to miR-330-3p overexpression (**Figure 3A**, **3B**), EREG knockdown (**Figure 4B**) and lncRNA-021545 knockdown (**Figure 5A**, **5B**), whereas, are reduced due to miR-330-3p knockdown (**Figure 3C**, **3D**) and EREG overexpression (**Figure 4A**).

MiR-330-3p has been reported to act as a tumor suppressing gene or oncogene or dual function roles in cancers [16-26, 29, 71]. Consistent with our work, miR-330-3p was reported to promote the proliferation, migration and invasion abilities of lung cancer A549, HCC827, NCI-H23, 95-C and 95-D cells [17, 27], the metastasis abilities of pancreatic cancer AsPC-1 cell [21], ESCC EC109 and KYSE-150 cells [18], the proliferation, migration, and invasion abilities of bladder cancer T24 and UM-UC-3 cells via downregulating RAI2 [25], the invasive abilities of breast cancer MDA-MB-231 cells [20], the migration and invasion [16, 23] of glioblastoma cells, the proliferation and invasion abilities of gastric cancer MKN-45, MGC-803 and HGC-27 cells [24, 72]. On the contrary, miR-330-3p has been shown as a tumor suppressor in a variety of cancers. It inhibited the migration and invasion abilities of ovarian cancer ES-2 cell by targeting RIPK4 [22], colorectal cancer SW480 and HT29 cell lines [26] by targeting PFN1 and laryngeal squamous cell carcinoma HEp-2 and AMC-HN-8 cells [71] by targeting Tra2β. Paradoxically, in glioma, miR-330-3p was reported to inhibit the migration and invasion of U251 cells by targeting CELF1 [63], while, to promote the migration and invasion of U87 and U251 cells by targeting SH3GL2 [16]. In liver cancer cells, miR-330-3p was reported to suppress the migration of HepG2 cells via targeting MAP2K1 [29], while, to enhance the migration and invasion of HCCLM3 cells via targeting BTG1 [20]. However, for both studies, only one hepatocarcinoma cell line was used, moreover, the effect of miR-330-3p overexpression in HCCLM3 was not performed. Herein, the combined results from both overexpressing and downregulating miR-330-3p in two hepatocarcinoma Huh7 and HCCLM3 cell lines concordantly demonstrated its promoting effects on their migration and invasion (**Figure 3A-D**). As miR-330-3p overexpression was already proved to be associated with clinical progression (**Figure 1B**), apparently, current work implicates miR-330-3p upregulation potentially increases HCC malignancy through promoting tumour cells' invasiveness.

EREG plays dual function roles in different cancers. It acts as a tumor suppressor in rectal and colorectal cancers [47, 48]. High EREG expression was related to less vascular and perineurial invasion, and higher tumor regression grade of rectal cancer patients with a favorable prognosis [47] and a longer overall survival of metastatic colorectal cancer patients administrated with oxaliplatin/fluoropyrimidine plus bevacizumab [48]. EREG acts as a tumor promoter in some cancers [39, 45, 69]. EREG increased the colony formation abilities of head and neck squamous cell carcinoma CAL27 and HN13 cells [39], the invasion and migration of oral squamous cell carcinoma HACAT and HSC3 cells [45], and the adhesion of colon cancer DLD-1 cells [69]. Consistent with current work, EREG was reported to increase the malignant behaviours (migration, invasion or adhesin) of HACAT, HSC3 and DLD-1 cells [45, 69] without affecting their proliferations. Few studies are available about EREG in liver cancer. So far, no study has been reported the protein expression level in tumorous specimens from liver cancer patients. In human liver cancer cell, EREG was involved in the decreased cell growths of HepG2 and Bel7402 synergistically induced by the dual knockdown of N-ras and EREG via ERK1/2 [49]. In DEN plus CCl_4-me-

diated hepatocarcinogenesis, a reduction of tumor number and size was obtained in EREG-deficient C57Bl/6 mice [46]. Little is known on EREG in liver cancer metastasis. Except for demonstrating EREG expression deficiency was linked to the clinical progression of hepatocarcinoma (**Figure 4A**), current work shows EREG expression inversely correlated with the migration and invasion of HCC cells (**Figure 4A**, **4B**). Therefore, EREG deficiency promotes HCC through increasing the migratory and invasive behaviours of tumour cells.

To date, current work is the earliest report on the associations of miR-330-3p and EREG with lncRNA021545 to form a circuit feedback mechanism in hepatocarcinoma metastasis. Except for the high lncRNA021545 expression that was detected in the peripheral blood of schizophrenic patients [38], the role and action mechanism of lncRNA021545 have not been touched. Our work here shows its deficiency with the clinical progression of hepatocarcinoma (**Figure 5**) and the migration and invasion abilities of HCC cells (**Figure 5A**, **5B**).

Collectively, all above evidences suggest a novel regulation mechanism in hepatocarcinogenesis, ie. miR-330-3p/lncRNA021545/EREG axis influences hepatocarcinoma malignancy through mediating the metastasis of hepatocarcinoma cells. We further showed that miR-330-3p/lncRNA021545/EREG affected hepatocarcinoma cells through EMT process. E-cadherin expression reduction and N-cadherin and vimentin expression enhancements are key mesenchymal indicators for cell undergoing EMT [73-75]. Snail and slug, two transcription factors (TFs), are commonly considered as the direct repressors of E-cadherin [75, 76]. We showed their expressions were changed in HCCLM3 and Huh7 cells in responding to the dysexpressions of miR-330-3p, EREG and lncRNA021545. MiR-330-3p level change inversely, while EREG and lncRNA021545 expression changes positively mediate E-cadherin expression in HCC cells (**Figure 6A-C**). Consistently, the expressions of N-cadherin, vimentin, snail and slug were found positively mediated by miR-330-3p dysexpression and inversely mediated by both EREG and lncRNA021545 alterations (**Figure 6A-C**). Here, our work first showed that miR-330-3p promoted HCC cell invasiveness through activating EMT progression. Consistently, miR-330-3p was reported to show promotion effect by decreasing E-cadherin expression and increasing N-cadherin, vimentin and snail expressions in lung cancer 95-C, 95-D, A549 and HCC827 cells [17, 77]. On the other hand, miR-330-3p was reported to upregulate E-cadherin and downregulate N-cadherin and vimentin in gastric cancer MKN-45 and MGC-803 cells [24]. Secondly, we linked EREG deregulation to the EMT of livre cancer cells. In oral squamous cell carcinoma HSC3 cells [45], EREG was reported to promote cancer-associated fibroblasts transition through up-regulating N-cadherin and vimentin. Here, interestingly in hepatocarcinoma, we showed EREG overexpression resulted in N-cadherin, vimentin, snail and slug reductions and E-cadherin increase in HCCLM3 cells, concordantly, EREG knockdown obtained the opposite results in Huh7 cells (**Figure 6A**), which indicated the direct EREG involvement in hepatocarcinoma EMT through mediating these proteins. Moreover, we proved miR-330-3p regulated HCC cell metastasis via EMT through EREG. In HCCLM3 cells, the increased migration and invasion, and the dysexpression changes of E-cadherin, N-cadherin, vimentin, snail and slug induced by miR-330-3p overexpression were reversed by EREG overexpression (**Figure 6D**, **6E**). MiR-330-3p only downregulated endogenous EREG expression by binding to its 3'-UTR, while could not decrease exogenous EREG overexpression by PCDH-EREG transfection for the lack of EREG-3'-UTR, concordantly, miR-330-3p overexpression in HCCLM3 by its mimic transfection could not decrease the migration and invasion abilities, and reverse the expressions of E-cadherin, N-cadherin, vimentin, snail and slug to same extents as measured in HCCLM3-PCDH-EREG cells (**Figure 6D**, **6E**). Finally, as no study has been reported about lncRNA021545 in cancer, current work for the first time reveals its suppressing role in liver cancer. LncRNA021545 knockdown apparently led to decreased E-cadherin expression and increased expressions of N-cadherin, vimentin, snail and slug in HCCLM3 and Huh7 cells (**Figure 6C**), which suggested its deficiency might enhance hepatocarcinoma through promoting HCC metastasis via activating EMT. The target competing bindings among miR-330-3p, EREG and lncRNA-021545 together with the mutual regulations of their expressions indicate that miR-330-3p/lncRNA021545/EREG affects hepatocarcinoma metastasis through EMT.

MiRNAs are considered as a core to ceRNA regulatory networks and an intermediate bridge between lncRNA and mRNA [68]. Therefore, we determined the ectopic dysexpression of miR-330-3p on the *in vivo* tumorigenicity and malignancy of HCCLM3 cells in nude mice. MiR-330-3p overexpression by its mimic transfection in HCCLM3 enhanced the tumor formation velocity and mass of xenograft implanted mice (**Figure 7A**). Correspondingly, miR-330-3p overexpression resulted in the apparent enlargements of the inguinal, pararenal and axillary LNs from HCCLM3-miR-330-3p-mimic group mice than HCCLM3-miR-NC mice (**Figure 7B**). HE assays showed that metastasis foci and cell clusters appeared in marginal sinus of inguinal and pararenal LNs of HCCLM3-miR-330-3p-mimic mice. The tumor cells adhered obviously with notable sinus infiltration, arranged disorderly in size, distributed with increasing nuclear/plasma ratio and clear intercellular heteromorphism. Some of the small lymphocytes appearing among tumor cells were surrounded by lymphoid follicles with expanded interfollicular area and enriched blood vessels (**Figure 7C**). Although might be due to the low expression and/or insufficient *in vivo* knockdown of miR-330-3p, no apparent tumor forming velocity, size and mass were observed for HCCLM3-miR-330-3p-inhibitor mice than HCCLM3-miR-NC mice (**Figure 7A**), the averaged masses of the dissected inguinal, pararenal and axillary LNs from HCCLM3-miR-330-3p-inhibitor group mice decreased significantly (**Figure 7B**). Strikingly, both the EREG and lncRNA021545 expressions were negatively corrected with miR-330-3p expressions in the primary tumorous tissues of different group mice. Compared with HCCLM3-miR-NC mice, miR-330-3p was upregulated and downregulated in the primary tumorous tissues from HCCLM3-miR-330-3p-mimic and HCCLM3-miR-330-3p-inhibitor group mice, correspondingly, the levels of EREG and lncRNA021545 were both significantly downregulated and upregulated with negative correlation significances with miR-330-3p changes, respectively (**Figure 8**). Here, consistent with their *in vitro* regulation mechanism in HCC cells and their expression pattern correlations in cancerous tissues from HCC patients, the *in vivo* xenograft nude mice experiment evidences further proved a novel miR-330-3p/lncRNA021545/EREG ceRNA regulation pathway in hepatocarcinoma progression. The *in vivo* animal experimental results further showed that miR-330-3p/lncRNA021545/EREG affect the carcinogenicity and metastasis of HCC cells through EMT invasion. N-cadherin, vimentin, snail and slug were upregulated and E-cadherin was downregulated in cancerous tissues from HCCLM3-miR-330-3p-mimic mice. Consistently, N-cadherin, vimentin, snail and slug were downregulated and E-cadherin was upregulated in cancerous tissues from HCCLM3-miR-330-3p-inhibitor mice (**Figure 9A**). Consistent with miR-330-3p dysexpression showing no influence on the *in vitro* proliferation of HCCLM3 and Huh7 cells (**Figure 3**), unchanged Ki-67 level among the three group mice (**Figure 9B**) also suggests that miR-330-3p mediates the *in vivo* tumorigenesis of Huh7 cells through affecting their invasive behaviours rather than proliferations.

Although miR-330-3p and EREG have been reported in cancers, the association in hepatocarcinoma malignancy is unavailable. Meanwhile, as a competing lncRNA for binding to EREG against miR-330-3p, the role and relevance of lncRNA021545 to miR-330-3p and EREG in cancer is blank. Current study reveals a novel ceRNA axis formed by lncRNA021545, miR-330-3p and EREG in regulating hepatocarcinoma though EMT, as schemed in **Figure 10**. In clinic, positively correlated in cancerous tissues from patients, the overall deficiencies of EREG and lncRNA021545 are reversely correlated with miR-330-3p overexpression in hepatocarcinoma progression. By direct bindings to EREG and lncRNA021545, miR-330-3p negatively regulates their expressions, lncRNA021545 knockdown results in EREG reduction and miR-330-3p upregulation, and EREG positively regulates lncRNA021545 without affecting miR-330-3p expression in HCC cancer cells. MiR-330-3p promotes, while EREG and lncRNA021545 suppress, the *in vitro* migratory and invasive behaviours of HCC cancer cells without affecting their proliferations. Further results show the dysexpressions of miR-330-3p, EREG and lncRNA021545 mediate the *in vitro* invasiveness of HCC cells through EMT process via affecting the expressions of E-cadherin, N-cadherin, vimentin, snail and slug. Nude mouse xenograft results indicate that miR-330-3p with inversely correlated expressions of EREG and lncRNA021545 promotes the *in vivo* tumorigenicity and metastasis of HCCLM3 cells via affecting the above indicators of EMT. Taken together, current work establishes a novel ceRNA regulation mecha-

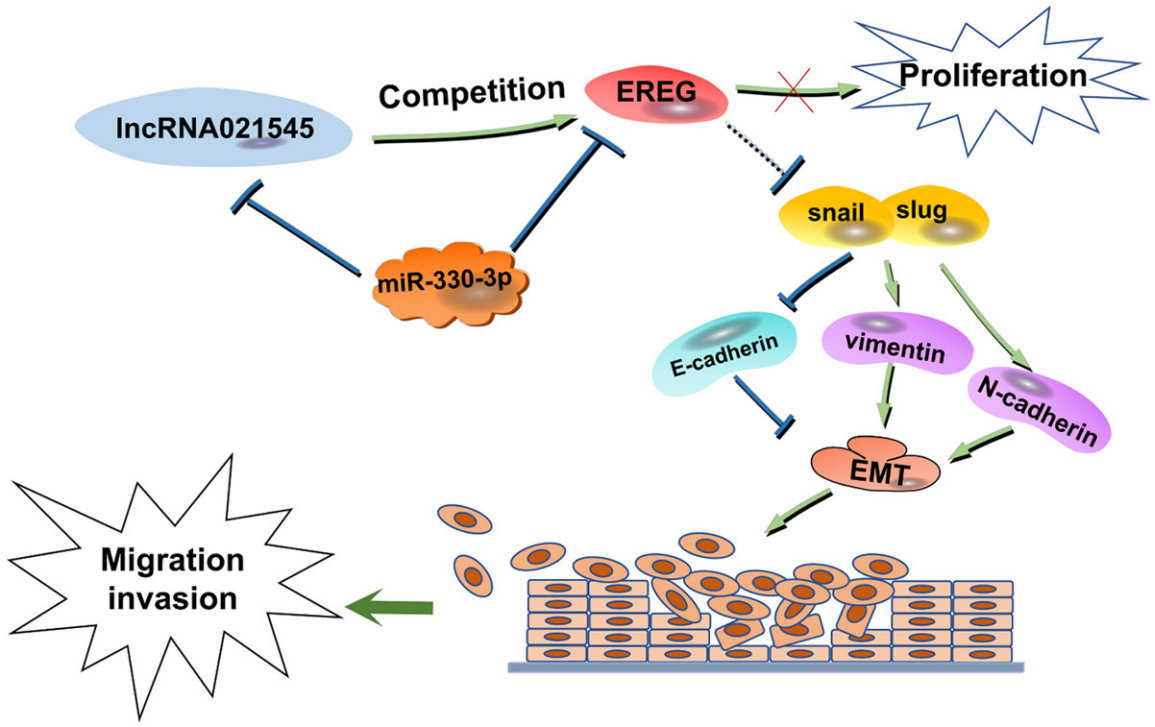

Figure 10. A graphic regulation illustration of miR-330-3p, lncRNA021545 and EREG in hepatocarcinoma malignancy. Forming a ceRNA circuit regulation relationship, the dysexpressions of the three molecules, miR-330-3p, lncRNA021545 and EREG play an important role in the clinal progression of hepatocarcinoma. Negatively correlated, the overexpression of miR-330-3p together with the deficiencies of lncRNA021545 and EREG interrupt the homeostatic feedback regulation, which then specifically enhance the migratory and invasive behaviours of tumor cells through activation EMT process, and finally promote hepatocarcinoma malignancy. Interestingly, it shows no influence on the proliferation of HCCLM3 cells. Pointed arrows indicate activation, blunt-ended lines indicate inhibition. Solid and dotted lines indicate direct and indirect activation/inhibition, respectively.

nism formed by miR-330-3p, lncRNA021545 and EREG in carcinogenesis.

In hepatocarcinoma, as shown in **Figure 10**, current work proposes that the imbalance of the overexpression of miR-330-3p together with the deficiencies of lncRNA021545 and EREG lead to the homeostasis interruption of miR-330-3p/lncRNA021545/EREG circuit regulation loop, which then contributes to the increasing malignant behaviours of hepatocarcinoma cells through promoting their metastatic abilities via EMT process and finally benefits the disease progression. It provides a novel fundamental clue as well as a potential appliable therapeutical target to the diagnosis and treatment of liver cancer.

Acknowledgements

This work was supported by grants from the National Natural Science Foundation of China (81672737), the Science Foundation of Liaoning Department of Education (LJKZ0284) and the Liaoning Provincial Program for Top Discipline of Basic Medical Sciences.

Disclosure of conflict of interest

None.

Address correspondence to: Qinlong Liu, Department of General Surgery, The Second Affiliated Hospital, Dalian Medical University, Dalian 116023, Liaoning, China. E-mail: qinlongliu@163.com; Shuqing Liu and Ming-Zhong Sun, College of Basic Medical Sciences, Dalian Medical University, Dalian 116044, Liaoning, China. E-mail: lsqsmz@163.com (SQL); smzlsq@163.com (MZS)

References

[1] Sung H, Ferlay J, Siegel RL, Laversanne M, Soerjomataram I, Jemal A and Bray F. Global cancer statistics 2020: GLOBOCAN estimates of incidence and mortality worldwide for 36 cancers in 185 countries. CA Cancer J Clin 2021; 71: 209-249.

[2] Ogunwobi OO, Harricharran T, Huaman J, Galuza A, Odumuwagun O, Tan Y, Ma GX and Nguyen MT. Mechanisms of hepatocellular carcinoma progression. World J Gastroenterol 2019; 25: 2279-2293.
[3] Guo C, Gao C, Zhao D, Li J, Wang J, Sun X, Liu Q, Hao L, Greenaway FT, Tian Y, Liu S and Sun MZ. A novel ETV6-miR-429-CRKL regulatory circuitry contributes to aggressiveness of hepatocellular carcinoma. J Exp Clin Cancer Res 2020; 39: 70.
[4] Tiwari N, Gheldof A, Tatari M and Christofori G. EMT as the ultimate survival mechanism of cancer cells. Semin Cancer Biol 2012; 22: 194-207.
[5] Puisieux A, Brabletz T and Caramel J. Oncogenic roles of EMT-inducing transcription factors. Nat Cell Biol 2014; 16: 488-494.
[6] Thiery JP, Acloque H, Huang RY and Nieto MA. Epithelial-mesenchymal transitions in development and disease. Cell 2009; 139: 871-890.
[7] Wu KJ and Yang MH. Epithelial-mesenchymal transition and cancer stemness: the Twist1-Bmi1 connection. Biosci Rep 2011; 31: 449-455.
[8] Zhang Q, Chai S, Wang W, Wan C, Zhang F, Li Y and Wang F. Macrophages activate mesenchymal stem cells to acquire cancer-associated fibroblast-like features resulting in gastric epithelial cell lesions and malignant transformation in vitro. Oncol Lett 2019; 17: 747-756.
[9] Nieto MA, Huang RY, Jackson RA and Thiery JP. EMT: 2016. Cell 2016; 166: 21-45.
[10] De Craene B and Berx G. Regulatory networks defining EMT during cancer initiation and progression. Nat Rev Cancer 2013; 13: 97-110.
[11] Yamada S, Okumura N, Wei L, Fuchs BC, Fujii T, Sugimoto H, Nomoto S, Takeda S, Tanabe KK and Kodera Y. Epithelial to mesenchymal transition is associated with shorter disease-free survival in hepatocellular carcinoma. Ann Surg Oncol 2014; 21: 3882-3890.
[12] Hou X, Yang L, Jiang X, Liu Z, Li X, Xie S, Li G and Liu J. Role of microRNA-141-3p in the progression and metastasis of hepatocellular carcinoma cell. Int J Biol Macromol 2019; 128: 331-339.
[13] Feng B, Zhu Y, Sun C, Su Z, Tang L, Li C and Zheng G. Basil polysaccharide inhibits hypoxia-induced hepatocellular carcinoma metastasis and progression through suppression of HIF-1α-mediated epithelial-mesenchymal transition. Int J Biol Macromol 2019; 137: 32-44.
[14] Hausser J and Zavolan M. Identification and consequences of miRNA-target interactions -- beyond repression of gene expression. Nat Rev Genet 2014; 15: 599-612.
[15] Liu J, Liu L, Chao S, Liu Y, Liu X, Zheng J, Chen J, Gong W, Teng H, Li Z, Wang P and Xue Y. The role of miR-330-3p/PKC-α signaling pathway in low-dose endothelial-monocyte activating polypeptide-II increasing the permeability of blood-tumor barrier. Front Cell Neurosci 2017; 11: 358.
[16] Qu S, Yao Y, Shang C, Xue Y, Ma J, Li Z and Liu Y. MicroRNA-330 is an oncogenic factor in glioblastoma cells by regulating SH3GL2 gene. PLoS One 2012; 7: e46010.
[17] Wei C, Zhang R, Cai Q, Gao X, Tong F, Dong J, Hu Y, Wu G and Dong X. MicroRNA-330-3p promotes brain metastasis and epithelial-mesenchymal transition via GRIA3 in non-small cell lung cancer. Aging (Albany NY) 2019; 11: 6734-6761.
[18] Meng H, Wang K, Chen X, Guan X, Hu L, Xiong G, Li J and Bai Y. MicroRNA-330-3p functions as an oncogene in human esophageal cancer by targeting programmed cell death 4. Am J Cancer Res 2015; 5: 1062-1075.
[19] Mesci A, Huang X, Taeb S, Jahangiri S, Kim Y, Fokas E, Bruce J, Leong HS and Liu SK. Targeting of CCBE1 by miR-330-3p in human breast cancer promotes metastasis. Br J Cancer 2017; 116: 1350-1357.
[20] Zhao X, Chen GQ and Cao GM. Abnormal expression and mechanism of miR-330-3p/BTG1 axis in hepatocellular carcinoma. Eur Rev Med Pharmacol Sci 2019; 23: 6888-6898.
[21] Xiong X, Shi Q, Yang X, Wang W and Tao J. LINC00052 functions as a tumor suppressor through negatively modulating miR-330-3p in pancreatic cancer. J Cell Physiol 2019; 234: 15619-15626.
[22] Cai L, Ye L, Hu X, He W, Zhuang D, Guo Q, Shu K and Jie Y. MicroRNA miR-330-3p suppresses the progression of ovarian cancer by targeting RIPK4. Bioengineered 2021; 12: 440-449.
[23] Zheng Z, Bao F, Chen X, Huang H and Zhang X. MicroRNA-330-3p expression indicates good prognosis and suppresses cell proliferation by targeting Bmi-1 in osteosarcoma. Cell Physiol Biochem 2018; 46: 442-450.
[24] Ma B, Ma J, Yang Y, He X, Pan X, Wang Z and Qian Y. Effects of miR-330-3p on invasion, migration and EMT of gastric cancer cells by targeting PRRX1-mediated Wnt/β-catenin signaling pathway. Onco Targets Ther 2020; 13: 3411-3423.
[25] Yang C, Mou Z, Zhang Z, Wu S, Zhou Q, Chen Y, Gong J, Xu C, Ou Y, Chen X, Dai X and Jiang H. Circular RNA RBPMS inhibits bladder cancer progression via miR-330-3p/RAI2 regulation. Mol Ther Nucleic Acids 2021; 23: 872-886.
[26] Huang Y, Sun H, Ma X, Zeng Y, Pan Y, Yu D, Liu Z and Xiang Y. HLA-F-AS1/miR-330-3p/PFN1 axis promotes colorectal cancer progression. Life Sci 2020; 254: 117180.

[27] Chen T, Yang Z, Liu C, Wang L, Yang J, Chen L and Li W. Circ_0078767 suppresses non-small-cell lung cancer by protecting RASSF1A expression via sponging miR-330-3p. Cell Prolif 2019; 52: e12548.
[28] Sun Y, Ma J, Lin J, Sun D, Song P, Shi L, Li H, Wang R, Wang Z and Liu S. Circular RNA circ_ASAP2 regulates drug sensitivity and functional behaviors of cisplatin-resistant gastric cancer cells by the miR-330-3p/NT5E axis. Anticancer Drugs 2021; 32: 950-961.
[29] Jin Z, Jia B, Tan L and Liu Y. miR-330-3p suppresses liver cancer cell migration by targeting MAP2K1. Oncol Lett 2019; 18: 314-320.
[30] Nagano T and Fraser P. No-nonsense functions for long noncoding RNAs. Cell 2011; 145: 178-181.
[31] Song YX, Sun JX, Zhao JH, Yang YC, Shi JX, Wu ZH, Chen XW, Gao P, Miao ZF and Wang ZN. Non-coding RNAs participate in the regulatory network of CLDN4 via ceRNA mediated miRNA evasion. Nat Commun 2017; 8: 289.
[32] Ørom UA and Shiekhattar R. Long noncoding RNAs usher in a new era in the biology of enhancers. Cell 2013; 154: 1190-1193.
[33] Morris KV and Mattick JS. The rise of regulatory RNA. Nat Rev Genet 2014; 15: 423-437.
[34] Cesana M, Cacchiarelli D, Legnini I, Santini T, Sthandier O, Chinappi M, Tramontano A and Bozzoni I. A long noncoding RNA controls muscle differentiation by functioning as a competing endogenous RNA. Cell 2011; 147: 358-369.
[35] Sun M, Nie F, Wang Y, Zhang Z, Hou J, He D, Xie M, Xu L, De W, Wang Z and Wang J. LncRNA HOXA11-AS promotes proliferation and invasion of gastric cancer by scaffolding the chromatin modification factors PRC2, LSD1, and DNMT1. Cancer Res 2016; 76: 6299-6310.
[36] Lin YH. Crosstalk of lncRNA and cellular metabolism and their regulatory mechanism in cancer. Int J Mol Sci 2020; 21: 2947.
[37] Hu X, Goswami S, Qiu J, Chen Q, Laverdure S, Sherman BT and Imamichi T. Profiles of long non-coding RNAs and mRNA expression in human macrophages regulated by interleukin-27. Int J Mol Sci 2019; 20: 6207.
[38] Chen S, Zhu X, Niu W, Yao G, Kong L, He M, Chen C, Lu Z, Cui X and Zhang L. Regulatory role of lncRNA NONHSAT089447 in the dopamine signaling pathway in schizophrenic patients. Med Sci Monit 2019; 25: 4322-4332.
[39] Liu S, Wang Y, Han Y, Xia W, Zhang L, Xu S, Ju H, Zhang X, Ren G, Liu L, Ye W, Zhang Z and Hu J. EREG-driven oncogenesis of head and neck squamous cell carcinoma exhibits higher sensitivity to erlotinib therapy. Theranostics 2020; 10: 10589-10605.
[40] Toyoda H, Komurasaki T, Uchida D, Takayama Y, Isobe T, Okuyama T and Hanada K. Epiregulin. A novel epidermal growth factor with mitogenic activity for rat primary hepatocytes. J Biol Chem 1995; 270: 7495-7500.
[41] He M, Jin Q, Chen C, Liu Y, Ye X, Jiang Y, Ji F, Qian H, Gan D, Yue S, Zhu W and Chen T. The miR-186-3p/EREG axis orchestrates tamoxifen resistance and aerobic glycolysis in breast cancer cells. Oncogene 2019; 38: 5551-5565.
[42] Thuong NT, Hawn TR, Chau TT, Bang ND, Yen NT, Thwaites GE, Teo YY, Seielstad M, Hibberd M, Lan NT, Caws M, Farrar JJ and Dunstan SJ. Epiregulin (EREG) variation is associated with susceptibility to tuberculosis. Genes Immun 2012; 13: 275-281.
[43] Verma V, Khoury S, Parisien M, Cho C, Maixner W, Martin LJ and Diatchenko L. The dichotomous role of epiregulin in pain. Pain 2020; 161: 1052-1064.
[44] Cai Y, Xie KL, Wu HL and Wu K. Functional suppression of epiregulin impairs angiogenesis and aggravates left ventricular remodeling by disrupting the extracellular-signal-regulated kinase1/2 signaling pathway in rats after acute myocardial infarction. J Cell Physiol 2019; 234: 18653-18665.
[45] Wang Y, Jing Y, Ding L, Zhang X, Song Y, Chen S, Zhao X, Huang X, Pu Y, Wang Z, Ni Y and Hu Q. Epiregulin reprograms cancer-associated fibroblasts and facilitates oral squamous cell carcinoma invasion via JAK2-STAT3 pathway. J Exp Clin Cancer Res 2019; 38: 274.
[46] Dapito DH, Mencin A, Gwak GY, Pradere JP, Jang MK, Mederacke I, Caviglia JM, Khiabanian H, Adeyemi A, Bataller R, Lefkowitch JH, Bower M, Friedman R, Sartor RB, Rabadan R and Schwabe RF. Promotion of hepatocellular carcinoma by the intestinal microbiota and TLR4. Cancer Cell 2012; 21: 504-516.
[47] Lin CY, Hsieh PL, Chou CL, Yang CC, Lee SW, Tian YF, Shiue YL and Li WS. High EREG expression is predictive of better outcomes in rectal cancer patients receiving neoadjuvant concurrent chemoradiotherapy. Oncology 2020; 98: 549-557.
[48] Stintzing S, Ivanova B, Ricard I, Jung A, Kirchner T, Tannapfel A, Juette H, Hegewisch-Becker S, Arnold D and Reinacher-Schick A. Amphiregulin (AREG) and epiregulin (EREG) gene expression as predictor for overall survival (OS) in oxaliplatin/fluoropyrimidine plus bevacizumab treated mCRC patients-analysis of the phase III AIO KRK-0207 trial. Front Oncol 2018; 8: 474.
[49] Zhao M, He HW, Sun HX, Ren KH and Shao RG. Dual knockdown of N-ras and epiregulin synergistically suppressed the growth of hu-

man hepatoma cells. Biochem Biophys Res Commun 2009; 387: 239-244.
[50] Zhong C, Yu Q, Peng Y, Zhou S, Liu Z, Deng Y, Guo L, Zhao S and Chen G. Novel LncRNA OXCT1-AS1 indicates poor prognosis and contributes to tumorigenesis by regulating miR-195/CDC25A axis in glioblastoma. J Exp Clin Cancer Res 2021; 40: 123.
[51] Goldring JPD. Measuring protein concentration with absorbance, lowry, bradford coomassie blue, or the smith bicinchoninic acid assay before electrophoresis. Methods Mol Biol 2019; 1855: 31-39.
[52] Rao X, Huang X, Zhou Z and Lin X. An improvement of the 2^(-delta delta CT) method for quantitative real-time polymerase chain reaction data analysis. Biostat Bioinforma Biomath 2013; 3: 71-85.
[53] Yuan JM, Wang Y, Wang R, Luu HN, Adams-Haduch J, Koh WP, Gao YT, Behari J and Lotze MT. Serum IL27 in relation to risk of hepatocellular carcinoma in two nested case-control studies. Cancer Epidemiol Biomarkers Prev 2021; 30: 388-395.
[54] Granata V, Grassi R, Fusco R, Belli A, Cutolo C, Pradella S, Grazzini G, La Porta M, Brunese MC, De Muzio F, Ottaiano A, Avallone A, Izzo F and Petrillo A. Diagnostic evaluation and ablation treatments assessment in hepatocellular carcinoma. Infect Agent Cancer 2021; 16: 53.
[55] Xu QG, Yu J, Guo XG, Hou GJ, Yuan SX, Yang Y, Yang Y, Liu H, Pan ZY, Yang F, Gu FM and Zhou WP. IL-17A promotes the invasion-metastasis cascade via the AKT pathway in hepatocellular carcinoma. Mol Oncol 2018; 12: 936-952.
[56] Lin Q, Zhou CR, Bai MJ, Zhu D, Chen JW, Wang HF, Li MA, Wu C, Li ZR and Huang MS. Exosome-mediated miRNA delivery promotes liver cancer EMT and metastasis. Am J Transl Res 2020; 12: 1080-1095.
[57] Reidy K and Susztak K. Epithelial-mesenchymal transition and podocyte loss in diabetic kidney disease. Am J Kidney Dis 2009; 54: 590-593.
[58] Derynck R and Weinberg RA. EMT and cancer: more than meets the eye. Dev Cell 2019; 49: 313-316.
[59] Brabletz T, Kalluri R, Nieto MA and Weinberg RA. EMT in cancer. Nat Rev Cancer 2018; 18: 128-134.
[60] Wang H, Chen SH, Kong P, Zhang LY, Zhang LL, Zhang NQ and Gu H. Increased expression of miR-330-3p: a novel independent indicator of poor prognosis in human breast cancer. Eur Rev Med Pharmacol Sci 2018; 22: 1726-1730.
[61] Yang Z, Wang W, Zhao L, Wang X, Gimple RC, Xu L, Wang Y, Rich JN and Zhou S. Plasma cells shape the mesenchymal identity of ovarian cancers through transfer of exosome-derived microRNAs. Sci Adv 2021; 7: eabb0737.
[62] Qian C, Chen S, Li S, Wang Y and Yao J. Circ_0000003 regulates glutamine metabolism and tumor progression of tongue squamous cell carcinoma via the miR-330-3p/GLS axis. Oncol Rep 2021; 45: 45.
[63] Wang H, Liu G, Li T, Wang N, Wu J and Zhi H. MiR-330-3p functions as a tumor suppressor that regulates glioma cell proliferation and migration by targeting CELF1. Arch Med Sci 2020; 16: 1166-1175.
[64] Stahler A, Heinemann V, Giessen-Jung C, Crispin A, Schalhorn A, Stintzing S, Fischer von Weikersthal L, Vehling-Kaiser U, Stauch M, Quietzsch D, Held S, von Einem JC, Holch J, Neumann J, Kirchner T, Jung A and Modest DP. Influence of mRNA expression of epiregulin and amphiregulin on outcome of patients with metastatic colorectal cancer treated with 5-FU/LV plus irinotecan or irinotecan plus oxaliplatin as first-line treatment (FIRE 1-trial). Int J Cancer 2016; 138: 739-746.
[65] Kogashiwa Y, Inoue H, Kuba K, Araki R, Yasuda M, Nakahira M and Sugasawa M. Prognostic role of epiregulin/amphiregulin expression in recurrent/metastatic head and neck cancer treated with cetuximab. Head Neck 2018; 40: 2424-2431.
[66] Wu X, Dong W, Zhang T, Ren H, Wang J, Shang L, Zhu Z, Zhu W, Shi X and Xu Y. Epiregulin (EREG) and myocardin related transcription factor A (MRTF-A) form a feedforward loop to drive hepatic stellate cell activation. Front Cell Dev Biol 2020; 8: 591246.
[67] Tomita K, Haga H, Mizuno K, Katsumi T, Sato C, Okumoto K, Nishise Y, Watanabe H, Saito T and Ueno Y. Epiregulin promotes the emergence and proliferation of adult liver progenitor cells. Am J Physiol Gastrointest Liver Physiol 2014; 307: G50-7.
[68] Salmena L, Poliseno L, Tay Y, Kats L and Pandolfi PP. A ceRNA hypothesis: the Rosetta Stone of a hidden RNA language? Cell 2011; 146: 353-358.
[69] Iijima M, Anai M, Kodama T and Shibasaki Y. Epiregulin-blocking antibody inhibits epiregulin-dependent EGFR signaling. Biochem Biophys Res Commun 2017; 489: 83-88.
[70] Han J, Qu H, Han M, Ding Y, Xie M, Hu J, Chen Y and Dong H. MSC-induced lncRNA AGAP2-AS1 promotes stemness and trastuzumab resistance through regulating CPT1 expression and fatty acid oxidation in breast cancer. Oncogene 2021; 40: 833-847.
[71] Cheng Y, Zhu H and Gao W. MicroRNA-330-3p represses the proliferation and invasion of laryngeal squamous cell carcinoma through downregulation of Tra2β-mediated Akt signaling. Mol Cell Probes 2020; 52: 101574.
[72] Guan A, Wang H, Li X, Xie H, Wang R, Zhu Y and Li R. MiR-330-3p inhibits gastric cancer pro-

gression through targeting MSI1. Am J Transl Res 2016; 8: 4802-4811.
[73] Eastham AM, Spencer H, Soncin F, Ritson S, Merry CL, Stern PL and Ward CM. Epithelial-mesenchymal transition events during human embryonic stem cell differentiation. Cancer Res 2007; 67: 11254-11262.
[74] Lamouille S, Xu J and Derynck R. Molecular mechanisms of epithelial-mesenchymal transition. Nat Rev Mol Cell Biol 2014; 15: 178-196.
[75] Peinado H, Marin F, Cubillo E, Stark HJ, Fusenig N, Nieto MA and Cano A. Snail and E47 repressors of E-cadherin induce distinct invasive and angiogenic properties in vivo. J Cell Sci 2004; 117: 2827-2839.
[76] Serrano-Gomez SJ, Maziveyi M and Alahari SK. Regulation of epithelial-mesenchymal transition through epigenetic and post-translational modifications. Mol Cancer 2016; 15: 18.
[77] Shen L, Yi S, Huang L, Li S, Bai F, Lei S, Breitzig M, Czachor A, Sun H, Zheng Q and Wang F. miR-330-3p promotes lung cancer cells invasion, migration, and metastasis by directly targeting hSOD2b. Biotechnol Appl Biochem 2019; 66: 21-32.